Atmos. Chem. Phys. Discuss., 10, 18507–18560, 2010
www.atmos-chem-phys-discuss.net/10/18507/2010/
doi:10.5194/acpd-10-18507-2010

Atmospheric Chemistry and Physics Discussions

Characterization of trace gases measured over Alberta oil sands mining operations: 76 speciated C_2–C_{10} volatile organic compounds (VOCs), CO_2, CH_4, CO, NO, NO_2, NO_y, O_3 and SO_2

I. J. Simpson[1], N. J. Blake[1], B. Barletta[1], G. S. Diskin[2], H. E. Fuelberg[3], K. Gorham[1], L. G. Huey[4], S. Meinardi[1], F. S. Rowland[1], S. A. Vay[2], A. J. Weinheimer[5], M. Yang[1,2], and D. R. Blake[1]

[1]Dept. of Chemistry, University of California-Irvine, Irvine, CA 92697, USA
[2]NASA Langley Research Center, Hampton, VA 23681, USA
[3]Dept. of Meteorology, Florida State University, Tallahassee, FL 32306, USA

[4]School of Earth & Atmospheric Sciences, Georgia Institute of Technology, Atlanta,
GA 30332, USA
[5]National Center for Atmospheric Research, 1850 Table Mesa Dr., Boulder, CO, 80305, USA

Received: 1 July 2010 – Accepted: 9 July 2010 – Published: 5 August 2010

Correspondence to: I. J. Simpson (isimpson@uci.edu)

Abstract

Oil sands comprise 30% of the world's oil reserves and the crude oil reserves in Canada's oil sands deposits are second only to Saudi Arabia. The extraction and processing of oil sands is much more challenging than for light sweet crude oils because of the high viscosity of the bitumen contained within the oil sands and because the bitumen is mixed with sand and contains chemical impurities such as sulphur. Despite these challenges, the importance of oil sands is increasing in the energy market. To our best knowledge this is the first peer-reviewed study to characterize volatile organic compounds (VOCs) emitted from Alberta's oil sands mining sites. We present high-precision gas chromatography measurements of 76 speciated C_2–C_{10} VOCs (alkanes, alkenes, alkynes, cycloalkanes, aromatics, monoterpenes, oxygenates, halocarbons, and sulphur compounds) in 17 boundary layer air samples collected over surface mining operations in northeast Alberta on 10 July 2008, using the NASA DC-8 airborne laboratory as a research platform. In addition to the VOCs, we present simultaneous measurements of CO_2, CH_4, CO, NO, NO_2, NO_y, O_3 and SO_2, which were measured in situ aboard the DC-8.

Methane, CO, CO_2, NO, NO_2, NO_y, SO_2 and 53 VOCs (e.g., halocarbons, sulphur species, NMHCs) showed clear statistical enhancements (up to 1.1–397×) over the oil sands compared to local background values and, with the exception of CO, were higher over the oil sands than at any other time during the flight. Twenty halocarbons (e.g., CFCs, HFCs, halons, brominated species) either were not enhanced or were minimally enhanced (<10%) over the oil sands. Ozone levels remained low because of titration by NO, and three VOCs (propyne, furan, MTBE) remained below their 3 pptv detection limit throughout the flight. Based on their mutual correlations, the compounds emitted by the oil sands industry fell into two groups: (1) evaporative emissions from the oil sands and its products and/or from the diluent used to lower the viscosity of the extracted bitumen (i.e., C_4–C_9 alkanes, C_5–C_6 cycloalkanes, C_6–C_8 aromatics), together with CO; and (2) emissions associated with the mining effort (i.e., CO_2, CO, CH_4, NO, NO_2, NO_y,

SO_2, C_2–C_4 alkanes, C_2–C_4 alkenes, C_9 aromatics, short-lived solvents such as C_2Cl_4 and C_2HCl_3, and longer-lived species such as HCFC-22 and HCFC-142b). Prominent in the second group, SO_2 and NO were remarkably enhanced over the oil sands, with maximum enhancements of 38.7 and 5.0 ppbv, or 383 and 319× the local background, respectively. The SO_2 enhancements are comparable to maximum values measured in heavily polluted megacities such as Mexico City and are attributed to coke combustion. By contrast, relatively poor correlations between CH_4, ethane and propane suggest low natural gas leakage despite its heavy use at the surface mining sites.

In addition to the emission of many trace gases, the natural drawdown of OCS by vegetation was absent above the surface mining operations, presumably because of the widespread land disturbance. Unexpectedly, the mixing ratios of α- and β-pinene were much higher over the oil sands (up to 217 and 610 pptv, respectively) than over vegetation in the background boundary layer (20±7 and 84±24 pptv, respectively), and the pinenes correlated well with several industrial tracers that were elevated in the oil sands plumes. Because so few independent measurements from the oil sands mining industry exist, this study provides an important initial characterization of trace gas emissions from oil sands surface mining operations.

1 Introduction

Hydrocarbons are the basis of oil, natural gas and coal. Crude oil contains hydrocarbons with five or more carbon atoms (i.e., $\geq C_5$), with an average composition of alkanes (30%), cycloalkanes (49%), aromatics (15%) and asphaltics (6%) (Alboudwarej et al., 2006). Oil sands comprise 30% of total world oil reserves (Alboudwarej et al., 2006) and are a mixture of sand, water, clay and crude bitumen – a thick, sticky extra-heavy crude oil that is "unconventional", i.e., does not flow and cannot be pumped without heating or dilution. With 179 billion barrels in its deposits, most of which occurs as oil sands, Canada has the world's 2nd largest crude oil reserves after Saudi Arabia and is currently the world's 7th largest producer of crude oil, generating about 1 million barrels day^{-1}, with almost 4 million barrels day^{-1} expected by 2020 (www.canadasoilsands.ca). Alberta is Canada's largest oil producer, with oil sands deposits in three relatively remote regions: Athabasca (which is serviced by Fort McMurray), Peace River, and Cold Lake (Fig. 1). Shallow oil sands deposits in the Athabasca region can be surface mined, which has disturbed about 500 km^2 of land and comprises ~20% of Alberta's oil sands production (www.oilsands.alberta.ca). Deeper deposits occur at all three sites and require other in situ recovery methods such as steam injection.

Oil sands processing extracts the bitumen from the oil sands and upgrades it into synthetic crude oil. The surface mining operators (e.g., Syncrude Canada, Suncor Energy, Albian Sands Energy) extract the bitumen using a hot water process that requires 34 m^3 of natural gas per barrel of bitumen (http://www.neb.gc.ca/clf-nsi/rnrgynfmtn/nrgyrprt/lsnd/pprtntsndchllngs20152006/qapprtntsndchllngs20152006-eng.html). Solvents/diluents are used to remove water and solids from the extracted bitumen and also decrease the bitumen's viscosity so that it can be piped to upgraders and refineries for processing. Diluent such as naphtha is used, which is a flammable liquid mixture of C_3–C_{14} hydrocarbons with major fractions of *n*-alkanes (e.g., heptanes, octane, nonane) and aromatics (e.g., benzene, toluene, ethylbenzene, xylenes) (Siddique et al., 2007). Paraffinic solvents/diluents may also be used, which consist of pentanes and hexanes (Siddique et al., 2006; D. Spink, personal communication, 2010). Upgraders crack and separate the bitumen into a number of fractions, e.g., fuel gas, synthetic crude oil, carbon (coke), and sulphur. There are upgraders at some of the surface mining sites north of Fort McMurray, at an in situ site south of Fort McMurray, and at downstream industrial centers such as the industrial heartland in Fort Saskatchewan, Alberta. Every 1 m^3 of oil sands generates 4 m^3 of tailings waste, which includes both residual bitumen and diluent (Siddique, 2006).

Despite the emerging importance of oil sands in the energy market, characterizations of the emissions of volatile organic compounds (VOCs) and other trace gases from the oil sands industry are extremely scarce in the peer-reviewed literature. Whereas downstream oil sands upgrading facilities can be monitored by ground-based studies (e.g., Mintz and McWhinney, 2008), independent studies of oil sands mining emissions are particularly difficult because the mining operations are not accessible to the public (Timoney and Lee, 2009). Instead, the majority of oil sands studies are reported in the so-called “grey literature”, consisting of discipline-specific reports, industrial monitoring reports, reports by industrially-controlled consortia, and reports commissioned by non-governmental organizations (Timoney and Lee, 2009). Air quality in the oil sands surface mining air shed is monitored locally by the Wood Buffalo Environmental Association (WBEA), which is a multi-stakeholder organization that represents industry, environmental groups, government, communities, and Aboriginal stakeholders. Long-term monitoring data and reports are available at the WBEA website (www.wbea.org) but these data have not been published in the peer-reviewed literature.

We present independent observations of 76 speciated C_2–C_{10} VOCs, sulphur dioxide (SO_2), carbon dioxide (CO_2), methane (CH_4), carbon monoxide (CO), ozone (O_3), nitric oxide (NO), nitrogen dioxide (NO_2), and total reactive nitrogen (NO_y=NO+NO_2+HNO_3+PANs+ other organic nitrates +HO_2NO_2+HONO+NO_3+2× N_2O_5+particulate NO_3^-+...) near surface oil sands mining and upgrading operations in Alberta’s Athabasca region. Although present in trace quantities in the Earth’s atmosphere, these gases drive the atmosphere’s chemistry and radiative balance (Forster et al., 2007 and references therein). For example hydrocarbons and nitrogen oxides (NO_x=NO+NO_2) are key atmospheric constituents that can react together in the presence of sunlight to form ground-level O_3, itself a greenhouse gas and air pollutant. Many hydrocarbons (e.g., benzene, toluene) can also be toxic or carcinogenic. Sulphur dioxide is produced by industrial processes including petroleum combustion and can contribute to photochemical smog and acid rain. Our measurements were made on 10 July 2008 during a 17-min boundary layer (BL) flight leg over the oil sands using the NASA DC-8 aircraft as a research platform (http://airbornescience.nasa.gov/platforms/aircraft/dc-8.html). The VOCs were collected in seventeen 45-s integrated whole air samples that were subsequently analyzed at the University of California, Irvine (UC-Irvine). The remaining trace gases were sampled continuously, with CO_2, CH_4, CO, NO, NO_2, NO_y, and O_3 reported every 1 s and SO_2 reported every 30 s. Although clearly limited in temporal and spatial extent, to our best knowledge these measurements represent the first independent characterization of speciated VOCs and many other trace gases from oil sands mining in the peer-reviewed literature.

2 Experimental

Boundary layer air was sampled over the Athabasca surface mines as part of the 2008 Arctic Research of the Composition of the Troposphere from Aircraft and Satellites (ARCTAS) field mission (http://www-air.larc.nasa.gov/missions/arctas/arctas.html). The summer deployment of ARCTAS was based in Cold Lake, Alberta (54°25′ N; 110°12′ W) and included eight 8-h science flights (Flights 17–24) from 29 June–13 July 2008. Although the major focus of the summer phase of ARCTAS was boreal biomass burning emissions (Jacob et al., 2010), on 10 July 2008 (Flight 23) there was an opportunity for the DC-8 to make two descents into the BL over northeast Alberta as part of a return transit flight from Thule, Greenland to Cold Lake (Fig. 2). During the first BL excursion (Leg 7) the DC-8 circled over the Athabasca oil sands mining area between 11:27–11:44 a.m. LT, at altitudes between 720–850 m and within an area bounded by 56°34′–57°09′ N and 111°01′–111°50′ W. Ten-day backward trajectories show that during Leg 7 the air masses arrived at the aircraft's pressure level from the west (Fig. 3a). The second BL run was flown shortly after, from 12:00–12:15 LT at altitudes between 980–1410 m (Leg 9). Flight leg 9 was an intercomparison leg between the DC-8 and the NASA P-3B aircraft that occurred in generally clean air approximately 1° further south (55°39′–56°16′ N and 112°44′–113°47′ W), i.e., not over the oil sands. The ten-day backward trajectories for Leg 9 show that the sampled air masses also arrived from the west and not from the oil sands mines to the north (Fig. 3b). Therefore, even though Leg 9 occurred at higher altitudes within the BL, we believe it provides a reasonable concurrent local background against which to compare the oil sands VOC enhancements (see additional discussion in Sect. 3.2.3).

2.1 Volatile organic compounds (VOCs)

2.1.1 Airborne whole air sampling

UC-Irvine has measured speciated VOCs from diverse environments for more than 30 years, using both ground-based and airborne platforms (e.g., Blake and Rowland, 1988, 1995; Colman et al., 2001; Blake et al., 2003, 2008; Katzenstein et al., 2003; Barletta et al., 2005, 2009; Simpson et al., 2002; 2006). Our sampling technique collects whole air samples (WAS) into 2-L electropolished, conditioned stainless steel canisters each equipped with a Swagelok Nupro metal bellows valve (Solon, OH). The electropolishing minimizes the surface area and any surface abnormalities, and the canister conditioning (baking the cans in humidified air at ambient pressure and 225°C for 12 h) forms an oxidative layer on the interior surface that further passivates the canister walls. The DC-8 payload included 168 of our 2-L air sampling canisters for each flight of the ARCTAS mission.

To prepare the canisters for field use, they are taken to the University of California Crooked Creek Station in the Sierra Nevada mountains (altitude=10 200 ft) for a pump-and-flush procedure that is repeated ten times, in which each canister is pressurized to 40 psig with ambient air and then vented to ambient pressure. Next the canisters are returned to our UC-Irvine laboratory where they are evacuated to 10^{-2} Torr and then pressurized to 1000 Torr with liquid nitrogen cleaned ultra-high purity helium, before a final evacuation to 10^{-2} Torr (E2M12 dual-stage vacuum pumps, Edwards Vacuum, Wilmington, MA). Lastly each canister is humidified by adding ~17 Torr of purified water (the approximate vapour pressure of water at room temperature) to minimize surface adsorption and improve the reproducibility of our analytical split ratios during laboratory analysis (see Sect. 2.1.2). Rigorous sensitivity tests have shown that alkene growth in our passivated canisters is limited to a maximum of 0.2 pptv day^{-1} and all other compounds reported here are stable over the typically short period that the cans are stored before analysis (Sive, 1998). By analyzing the Alberta samples within 7 days of collection, we were able to limit the size of any alkene artefact to 1.4 pptv or less (i.e., to negligible values).

During each flight the whole air sampling is manually controlled and uses a stainless steel double bellows pump (MB-602, Senior Aerospace Metal Bellows, Sharon, MA) to draw outside air into a window-mounted 1/4 in. forward-facing inlet, through our air sampling manifold, and into one of the 168 canisters until it is filled to 40 psig. During Leg 7 we collected seventeen 45-s air samples, or approximately one sample per minute. During Leg 9 we collected 1-min integrated air samples every 3 min, for a total of 6 samples.

2.1.2 Laboratory analysis of VOCs

After Flight 23 the whole air samples were returned to our UC-Irvine laboratory for analysis using three gas chromatographs (GCs) coupled with a suite of detectors that together are sensitive to the 76 C_2–C_{10} VOCs that we seek to measure. We use two flame ionization detectors (FIDs) to measure hydrocarbons, two electron capture detectors (ECDs) for halocarbons, and a quadrupole mass spectrometer detector (MSD) for sulphur compounds.

Complete analytical details are given in Colman et al. (2001). For each sample a 1520 cm^3 sample aliquot is introduced into the analytical system's manifold and passed over glass beads contained in a loop maintained at liquid nitrogen temperature. A Brooks Instrument mass flow controller (model 5850E) keeps the flow below 500 $cm^3\ min^{-1}$ to ensure complete trapping of the less volatile sample components (e.g., VOCs) while allowing more volatile components (e.g., N_2, O_2, Ar) to be pumped away. The less volatile species are re-volatilized by immersing the loop in hot water (80 °C) and are then flushed into a helium carrier flow. The sample flow is split into five streams, with each stream chromatographically separated on an individual column and sensed by a single detector, namely: (1) FID with a DB-1 column (60 m, I.D. 0.32 mm, film 1 mm); (2) FID with PLOT (30 m, I.D. 0.53 mm)+DB-1 (5 m, I.D. 0.53 mm, film 1 mm) columns; (3) ECD with a Restek 1701 column (60 m, I.D. 0.25 mm, film 0.50 mm);

(4) ECD with DB-5 (30 m, I.D. 0.25 mm, film 1 mm)+Restek 1701 (5 m, I.D. 0.25 mm, film 0.5 mm) columns; and (5) MSD with a DB-5ms column (60 m, I.D. 0.25 mm, film 0.5 mm). The split ratios are highly reproducible as long as the specific humidity of the injected air is above 2 g-H_2O/kg-air, which we ensure by adding purified water into each canister (Sect. 2.1.1). The signal from each FID and ECD is output to a personal computer and digitally recorded using Chromeleon Software; the MSD output signal uses Chemstation software. To ensure that the measurements are of the highest calibre, each peak of interest on every chromatogram is individually inspected and manually modified. For Flight 23 more than 10 000 peaks were hand-modified.

Calibration is an ongoing process whereby new standards are referenced to older certified standards, with appropriate checks for stability and with regular inter-laboratory comparisons. Multiple standards are used during sample analysis, including working standards (analyzed every four samples) and absolute standards (analyzed twice daily). Here we used working standards collected in the Sierra Nevada mountain range. International intercomparison experiments have demonstrated that our analytical procedures consistently yield accurate identification of a wide range of unknown hydrocarbons and produce excellent quantitative results (e.g., Apel et al., 1999, 2003). Table 1 shows the measurement precision, accuracy and detection limit for each VOC. Even though our detection limit is conservative, the accuracy and precision of many species does deteriorate as we approach this limit.

2.2 SO_2, CO_2, CH_4, CO, NO, NO_2, NO_y, O_3

In addition to VOCs measured by UC-Irvine, we also present SO_2, CO_2, CO, CH_4, NO, NO_2, NO_y, and O_3 mixing ratios, which were measured in situ aboard the DC-8 by four research teams each using fast-response, high precision, continuous real-time instruments. The measurement precision and accuracy of these compounds are given in Table 1. The time response is 1 s for all compounds except NO and NO_2, which have a 3 s time response (SO_2 has a 1 s time response but was reported as a 30 s average). Briefly, SO_2 was measured using the Georgia Tech Chemical Ionization Mass

Spectrometer (GT-CIMS) instrument, which uses SF_6^- ion chemistry to selectively ionize SO_2 (Kim et al., 2007). Carbon dioxide CO_2 was measured using the NASA Langley Atmospheric Vertical Observations of CO_2 in the Earth's Troposphere (AVOCET) instrument, which uses a modified Li-Cor model 6252 differential, non-dispersive infrared (NDIR) gas analyzer at the 4.26 µm CO_2 absorption band (Vay et al., 1999, 2003). Methane and CO were measured by the NASA Langley Differential Absorption CO Measurement (DACOM) instrument, which uses two tunable diode lasers in the infrared spectral region to simultaneously measure the absorption of light by CH_4 (3.3 µm) and CO (4.7 µm) (Fried et al., 2008). Nitric oxide, NO_2, NO_y, and O_3 were measured using the 4-channel NCAR $NO_{xy}O_3$ chemiluminescence instrument (Weinheimer et al., 1994).

3 Results and discussion

Mixing ratio time series for Flight 23 are shown for selected species in Figs. 4 and 10, and altitudinal profiles are shown for many measured species in Figs. 5–9. Measurement statistics for Flight 23 – including the BL excursions over oil sands mining (Leg 7, n=17) and in background air (Leg 9, n=6) – are given in Table 1. For comparison, statistics for free troposphere (FT) measurements made earlier in the flight are also shown (60–76° N; n=66). Results for individual samples collected during Leg 7 (Table 2) show that not all of these samples were influenced by emissions from the oil sands because some samples were collected south of the surface mining sites as the plane manoeuvred (Fig. 2b). For many compounds their maximum enhancements were measured directly downwind of the Syncrude Mildred Lake Facility (i.e., samples 4–6 in Table 2 and Fig. 2b). For other compounds such as isoprene, which has a dominant biogenic source, its maximum occurred further south over vegetation (i.e., sample 14). Because the Leg 7 samples ranged from near-background air to strongly polluted industrial plumes, the discussion below includes a "maximum enhancement" over the Leg 9 background average, based on each compound's maximum mixing ratio during Leg 7. For correlation purposes, the SO_2, CO_2, CH_4, CO, NO, NO_2, NO_y and O_3 data are based on the average only of those 1 s measurements (30 s for SO_2) that overlapped the VOC sampling times (i.e., the so-called hydrocarbon data merge). The complete 1 s and 30 s data sets for these eight compounds, together with all the VOC data from the summer phase of ARCTAS, are at ftp://ftp-air.larc.nasa.gov/pub/ARCTAS/DC8_AIRCRAFT/.

3.1 General features

Atmospheric trace gas mixing ratios are generally higher in the Earth's BL than above in the FT, and the observed mixing ratio patterns for Flight 23 can be separated into three groups: (1) compounds that only increased during the descent over the oil sands; (2) compounds that increased during both BL runs; and (3) compounds that did not increase during either BL run (i.e., neither over the oil sands nor in background air), or else showed only small enhancements (<10%) over the oil sands. The first group, easily the largest, includes SO_2, NO, NO_2, NO_y, CO_2, CH_4, CO, and 70% of the measured VOCs, namely alkanes, aromatics, cycloalkanes, alkenes, oxygenates, ethyne, short-lived solvents (C_2Cl_4, C_2HCl_3, $CHCl_3$, CH_2Cl_2) and some HCFCs (Sects. 3.2, 3.3.3 and 3.4–3.6). The maximum enhancements were 1.1–397× the background BL values, most notably *n*-heptane (397×), SO_2 (382×), NO (319×), *n*-octane (242×), NO_2 (210×), *m*+*p*-xylene (181×) and methylcyclohexane (113×). The second group comprises biogenic tracers (i.e., isoprene and α- and β-pinene), though interestingly their increases were larger over the oil sands than in the background BL air, especially for the pinenes (Sect. 3.2.3). In the third group, long-lived industrial halocarbons (e.g., CFCs, CCl_4, CH_3CCl_3), several brominated species, and ozone (O_3) were not enhanced over the oil sands (Sects. 3.3.1 and 3.5). In fact O_3 was relatively depleted because of titration by high levels of NO. Halocarbons including HFC-134a, HCFC-141b, the halons and the methyl halides were minimally enhanced over the oil sands (Sect. 3.3.2).

Before discussing the results below, it is important to first recognize the limitations of this data set. Because of its short time-frame (17 min) and sample size ($n=17$), the representativeness of the measured VOC enhancements is unclear. On the other hand, because emissions from oil sands mining are so poorly characterized in the peer-reviewed literature due to the inaccessibility of mining sites to independent observers, this study provides important close-range observations of the VOCs that are being released, i.e., which individual species are emitted and with what other species do they correlate. The large number of compounds and relatively small number of samples in this data set make it unsuitable for emission estimates or for factor analysis such as Principal Component Analysis or Positive Matrix Factorization (e.g., Thurston and Spengler, 1985; Paatero, 1997; Choi et al., 2003), and we have instead performed simple correlations among the measured species to better understand their source influences.

3.2 Nonmethane hydrocarbons (NMHCs)

Nonmethane hydrocarbons (NMHCs) are mainly emitted from three major sources: vegetation, biomass burning, and anthropogenic activities such as industry and fossil fuel production, distribution and combustion (Guenther et al., 2000; Ehhalt and Prather, 2001; Folberth et al., 2006). Remarkably, of the 48 C_2–C_{10} hydrocarbons that we measured, all but three (propyne, furan, MTBE) showed very strong enhancements over the oil sands (maximum values at least 80% more than the local background average). Based on their mutual correlations, the NMHCs appear to have two distinct sources: (1) the oil sands and its products and/or the diluent used to lower the viscosity of the extracted bitumen (enhanced levels of C_4–C_9 alkanes, C_5–C_6 cycloalkanes, C_6–C_8 aromatics), and (2) industrial sources that support the mining effort, such as upgrading (elevated levels of C_2–C_4 alkanes, C_2–C_4 alkenes, C_9 aromatics).

3.2.1 Alkanes, cycloalkanes, aromatics

Because of increasing reactivity with the hydroxyl radical (OH) with increasing chain length, the average (±1σ) *n*-alkane mixing ratios decreased with increasing chain length in the background BL (Leg 9), from ethane (781±22 pptv) to propane (200±26 pptv) to *n*-butane (63±19 pptv), etc. (Table 1). The $\geq C_7$ *n*-alkanes are so short-lived (<2 days) that they were undetectable in the background BL (< 3 pptv). By contrast, all 12 C_2–C_9 alkanes were strongly enhanced in the oil sands plumes. Maximum ethane (1490 pptv) and propane (714 pptv) levels occurred in sample 4 downwind of the Syncrude Mildred Lake Facility (Fig. 2b) and were almost double and quadruple the background BL values, respectively (Table 1; Fig. 5a and b). Despite minimal urbanization in northern Alberta, the oil sand plume values were comparable to average ethane and propane levels measured in Baltimore and New York City during a summer study of 28 US cities from 1999–2005 (Baker et al., 2008). However they were smaller than median values measured during summer 2006 in the Houston and Galveston Bay area, which is both a large urban area and a major petrochemical manufacturing center (ethane, 4407 pptv; propane 2713 pptv) (Gilman et al., 2009). The primary ethane and propane sources are fossil fuel production (mainly unburned gas in the case of ethane), biofuel, and biomass burning, and propane is also emitted in gasoline exhaust (e.g., Watson et al., 2001; Buzcu and Fraser, 2006; Xiao et al., 2008). Ethane and propane correlated well with a range of species such as other light alkanes, alkenes, NO, NO_2, NO_y, and ethyne (Table 3). Because ethane and propane are primarily associated with evaporative rather than combustive fossil fuel emissions, we expect a co-located evaporative source from the industries that process the oil sands. Ethane is the second most abundant component of natural gas after CH_4 (Xiao et al., 2008), and the relatively poor correlation between ethane and CH_4 (r^2=0.52) is surprising given the heavy use of natural gas during bitumen extraction (Sect. 1) and may indicate low natural gas leakage levels.

The butanes are associated with fossil fuel evaporation (i.e., unburned gas) and biomass burning (Blake et al., 1996; Watson et al., 2001; Buzcu and Fraser, 2006). Maximum values over the oil sands were 10–12 times higher than in the background BL (Table 1; Fig. 5c) and the *i*-butane maximum was the highest recorded throughout the entire summer phase of ARCTAS. The *i*-butane (290 pptv) and *n*-butane (765 pptv) maxima in the oil sands plumes were similar to the lower range of values measured in the 28 US city study (Baker et al., 2008) and were comparable to maximum levels measured in fresh biomass burning plumes during ARCTAS (not shown). Interestingly, even though they only contain 4 carbon atoms, the butanes correlated better with the suite of heavier compounds that is associated with direct emissions from the oil sands and/or diluent (e.g., *n*-hexane, xylenes, cyclopentane; $0.93 \le r^2 \le 0.96$) than with species linked to industrial activities associated with the mining operations (e.g., propane, $CHCl_3$, ethene, ethyne, NO, NO_y; $0.77 \le r^2 \le 0.84$) (Table 3). Because the butanes are not generally associated with combustive fossil fuel emissions, these results indicate multiple evaporative butane sources at the mining sites.

Crude oil is composed of $\ge C_5$ alkanes, aromatics, cycloalkanes and asphaltics (Sect. 1), and even though the oil sands are extra-heavy and include molecules with 50 or more carbon atoms, they are still expected to contain a certain fraction of volatiles that would be captured by our measurements (D. Spink, personal communication, 2010). The C_5–C_9 *n*-alkanes showed very strong enhancements, with higher values over the oil sands than at any other time during the summer phase of ARCTAS. It is noteworthy that the maximum abundances were not ordered according to chain length. *n*-Heptane (596 pptv) showed the highest maximum mixing ratio, followed by the pentanes (510–560 pptv), *n*-octane (363 pptv) and *n*-hexane (294 pptv) (Table 1; Figs. 4c and 5d–f). These values represent enhancements of 24–397 times the background BL values (a background value of 1.5 pptv was assumed for BL measurements that were below our detection limit of 3 pptv). Oil having a plant origin is known to show a predominance for *n*-alkanes with an odd chain number, in contrast to *n*-alkanes that are produced from marine organic matter (Rogers and Koons, 1971). Because oil sands are derived from marine phytoplankton, the relative abundance of pentanes and *n*-heptane may suggest a stronger signal from the diluent than from the oil sands, assuming the diluent is made from conventional plant-based oil. Branched alkanes such as 2,3-dimethylbutane and the methylpentanes (which we present as a single measurement, i.e., 2+3-methylpentane) were also enhanced by factors of 19–34 over the local background (Table 1).

The cycloalkanes were close to or below our 3 pptv detection limit during Leg 9, as they had been in the FT during the transit from Thule. By contrast, all the cycloalkanes were strongly enhanced over the oil sands, with maximum mixing ratios ranging from 41 pptv (cyclopentane) to 339 pptv (methylcyclohexane) (Table 1; Figs. 4e and 6a). Cycloalkanes are a major component of crude oil (Sect. 1), and these results are consistent with their evaporative release from oil sands surface mining operations.

Aromatics are associated with combustion (fossil fuel and biomass burning), fuel evaporation, industry and biogenic emissions (e.g., Karl et al., 2009a; White et al., 2009). With the exception of the longest-lived aromatics that we measured – i.e., benzene (1–2 weeks) and toluene (2–3 days) – none of the aromatics were detectable in either the FT or in background BL air, whereas they were all strongly elevated over the oil sands with maximum enhancements of 7–181× over the background BL (Table 1; Figs. 4f and 6b–d). Toluene was the most abundant aromatic in the oil sands plumes (401 pptv maximum) followed by the xylenes (127–272 pptv) and benzene (82 pptv). For comparison these aromatic enhancements are much smaller than the maximum values measured near major petrochemical complexes in urban/industrial areas of Houston, Texas and southern Catalonia, Spain (e.g., toluene maxima of 16 000–77 000 pptv; Gilman et al., 2009; Ras et al., 2009). That is, the release of aromatics from the oil sands mining sites appears to be much smaller than releases further downstream during petrochemical refining.

With the exception of the C_9 aromatics, the $\geq C_5$ alkanes, cycloalkanes and aromatics show excellent mutual correlations (Table 3). Interestingly, the best correlations were not limited to compounds within the same class, but were mixed among the compound classes. For example, *n*-heptane, the most strongly enhanced VOC, showed top 10 correlations with *n*-nonane, *n*-octane, toluene, methylcyclopentane, *n*-hexane, benzene, cyclohexane, 2+3-methylpentane, *m*+*p*-xylene, and ethylbenzene ($0.95 \le r^2 \le 0.99$). These results show the fugitive co-emissions of a wide range of C_5–C_9 VOCs from oil sands surface mining sites in Alberta. By contrast, the C_9 aromatics (i.e., ethyltoluenes, trimethylbenzenes) correlated best with each other and with combustion and industrial tracers such as NO, NO_2, NO_y, ethene, propene and *cis*-2-butene, suggesting their release from industries at the mining sites as opposed to direct evaporative release from the oil sands and/or diluent.

3.2.2 Alkenes, alkynes

Because it is a biogenic tracer, isoprene is considered separately below (Sect. 3.2.3). The 7 C_2–C_4 alkenes considered here are highly reactive, short-lived compounds that are associated with industrial emissions and incomplete combustion (e.g., Sprengnether et al., 2002; Buzcu and Fraser, 2006; de Gouw et al., 2009). Whereas only ethene was detectable in the background BL during Flight 23 (20±2 pptv), all of the alkenes were strongly enhanced over the oil sands, by factors of up to 5–85 over their background mixing ratios (Table 1; Figs. 4g and 6e). The maximum mixing ratio decreased with increasing chain length, from ethene (270 pptv) to propene (128 pptv) to *i*-butene (37 pptv), etc. Although these oil sands values are much larger than the rural background, they are lower for example than in fresh biomass burning plumes encountered during ARCTAS (e.g., ethene up to 18 690 pptv, propene up to 5465 pptv). They are also in the low range of summertime values in US cities (e.g., ethene, 260–2430 pptv; propene 68–500 pptv; *i*-butene 33–1550 pptv; Baker et al., 2008). In the Houston area – where the greatest concentration of petrochemical facilities in the US is located and ethene and propene play a major role in rapid O_3 formation (Ryerson et al., 2003) – average respective ethene and propene mixing ratios of 2690 and 1540 pptv were measured in summer, 2006 (Gilman et al., 2009), and poor correlation between ethene and CO suggested the dominance of industrial point sources (de Gouw et al., 2009). Over the oil sands, ethene showed excellent correlation with the combustion tracer ethyne (r^2=0.96), some correlation with CO (r^2=0.6), and good correlation with the industrial tracer C_2Cl_4 (r^2=0.79) (Table 3), suggesting the mixed influence of industrial and combustion sources on ethene and other alkenes at the oil sands mining sites.

Propyne was not detectable in any of the samples that we collected during Flight 23. Ethyne – a tracer of incomplete combustion by biomass burning and urban fossil fuel (Blake et al., 2003; Warneke et al., 2007) – correlated most strongly with ethene, NO_y, NO and the trimethylbenzenes ($0.91 \le r^2 \le 0.96$) and showed a maximum mixing ratio of 138 pptv over the oil sands, compared to 59±5 pptv in the local background (Table 1; Fig. 6f). As with the alkenes, this enhancement is small compared to average levels measured in Houston (473 pptv; Gilman et al., 2009) and in the 28 US city study (260–2390 pptv; Baker et al., 2008), indicating the relatively low impact of industrial combustion on the measured ethyne levels.

3.2.3 Isoprene, monoterpenes

Isoprene (C_5H_8) is a short-lived (~2.8 h) biogenic volatile organic compound (BVOC) with a major terrestrial plant source. Isoprene levels vary widely in North America, with greatest emission rates in the Eastern US during summer (Guenther et al., 2006). For example in the 28 US city study the lowest average isoprene mixing ratio was measured in El Paso, Texas (47±75 pptv) and the highest in Providence, Rhode Island (2590±1610 pptv) (Baker et al., 2008). In our study, isoprene mixing ratios exceeded 200 pptv in all 17 air samples collected over the oil sands and in the local background air. Interestingly, the average isoprene mixing ratio was 50% greater during Leg 7 (468±147 pptv) than in the local background air (311±95 pptv), with a maximum value of 780 pptv (Tables 1 and 2; Fig. 4h). Anthropogenic sources of isoprene include traffic (e.g., Reimann et al., 2000; Borbon et al., 2001; Barletta et al., 2002) and industry (e.g., Ras et al., 2009). However the isoprene maximum was measured in sample 14, south of the main surface mining operations. Isoprene was poorly correlated with all of the trace gases that we measured ($r^2<0.37$) and its enhancements appear to be biogenic rather than industrial in origin. We believe that the stronger enhancements during Leg 7 than Leg 9 most likely reflect natural source strength variability rather than an altitude effect. Isoprene is highly reactive with OH and it is the shortest-lived species that we measure (Table 1). Although the Leg 7 samples were collected at a lower average altitude (804±38 m) than the background BL measurements (1135±180 m) (Sect. 2) – and in principle more isoprene oxidation by OH could have occurred during transport to higher altitudes during Leg 9 – the individual measurements did not show a clear declining trend with altitude.

Like isoprene, monoterpenes ($C_{10}H_{16}$) are short-lived (~3.7–5.3 h) BVOCs that are emitted by vegetation, though in this case they are more strongly emitted by coniferous ecosystems than by temperate deciduous forests (Fuentes et al., 2000). During this study the pinenes were enhanced during both BL runs compared to measurements in the FT (Fig. 7a and b). Interestingly, however, the maximum α- and β-pinene mixing ratios over the oil sands (217 pptv and 610 pptv, respectively) were 7–11× greater than their respective average values in the background BL air (20±7 and 84±24 pptv; Table 1, Fig. 7a and b). At first glance this appears to be consistent with findings by Schade and Goldstein (2003) in which monoterpene mixing ratios and emissions from a California ponderosa pine forest showed a 10–30 fold increase during and after major forest thinning, with measured mixing ratios exceeding 3000 pptv. However, unlike isoprene, the pinenes were most strongly enhanced in sample 4, downwind of the Syncrude Mildred Lake Facility (Table 2; Fig. 2b) and they showed strong correlations with many species that were elevated in the oil sands plumes. For example α-pinene correlated best with β-pinene (r^2=0.92), C_2Cl_4 (r^2=0.81), SO_2 (r^2=0.76), 1,2,3-TMB (r^2=0.74), *i*-butene (r^2=0.73) and ethyne (r^2=0.73). These unexpected observations lead us to infer that there could be a source of pinenes associated with the oil sands mining industry, which requires further investigation.

3.2.4 Oxygenates

During ARCTAS UC-Irvine measured methanol, ethanol, acetone, methyl ethyl ketone (MEK), methacrolein (MAC), methyl vinyl ketone (MVK), methyl *tert*-butyl ether (MTBE), and furan. Oxygenate sources are both natural and anthropogenic and include vegetation, industry, biomass burning and the oceans (e.g., Horowitz et al., 2003; Folberth et al., 2006 and references therein). In terms of anthropogenic sources, MTBE is a solvent and gasoline additive in many parts of the world, and the remaining oxygenates that we measured have a variety of applications in industry such as solvents or intermediates in the chemical synthesis of polymers, resins, etc.

The impact of oil sands emissions on the measured oxygenate levels varied widely. Both furan and MTBE remained below our detection limit of 3 pptv throughout Flight 23, and the remaining compounds showed a range of enhancements over the oil sands (Table 1; Fig. 7c–f). The shorter-chained, longer-lived species (methanol, ethanol, acetone) were enhanced by factors of 1.8–1.9 over the oil sands compared to the local background, and these mixing ratios were comparable to those measured at higher altitudes and latitudes during earlier portions of the flight. By comparison, the longer-chained, shorter-lived oxygenates (MEK, MAC and MVK) showed higher mixing ratios over the oil sands than at any other time during the flight, with maximum values of 214–379 pptv or 6–11 times the local background.

Methanol correlated best with MEK and the butenes ($0.71 \leq r^2 \leq 0.75$), ethanol with CH_3CCl_3 and the halons ($0.65 \leq r^2 \leq 0.83$), and acetone with MAC, 1,2-dichloroethane and CH_2Cl_2 ($0.64 \leq r^2 \leq 0.69$), suggesting their co-release with other industrial compounds used during mining operations. Note that even though methanol has a strong biogenic source (Jacob et al., 2005 and references therein) that was evident at other times during the summer phase of ARCTAS (not shown), it did not correlate with isoprene during Leg 7 ($r^2 < 0.01$). MEK also showed strong correlations ($r^2 > 0.8$) with a dozen industrial and combustion tracers including C_2–C_4 alkenes, C_2Cl_4, NO and 1,2,3-TMB. By contrast, MAC and MVK correlated most strongly with each other

(r^2=0.87), followed by species such as DMS and 1,2-DCE ($r^2 \leq 0.69$). MAC and MVK are major isoprene oxidation products (e.g., Karl et al., 2009b), and their strongest correlations with each other suggest that their primary local source is isoprene oxidation.

3.3 Halocarbons

Long-lived halocarbons (e.g., CFCs, HCFCs) contribute to stratospheric ozone depletion, and short-lived halocarbons (e.g., $CHCl_3$, C_2Cl_4) can be toxic or carcinogenic. Of the 26 C_1–C_2 halocarbons that we measured, 6 showed both strong (≥10%) enhancements over the local background average and larger mixing ratios over the oil sands than at any other time during the flight, 9 showed minimal enhancements over the local background average, and 11 were not statistically enhanced over the oil sands.

3.3.1 Strongly enhanced halocarbons

The first group includes the CFC-substitutes HCFC-22, HCFC-142b, and the relatively short-lived (2–5 mo) industrial solvents chloroform ($CHCl_3$), trichloroethene (C_2HCl_3), tetrachloroethene (C_2Cl_4), and methylene chloride (CH_2Cl_2). HCFC-22 and HCFC-142b are long-lived refrigerants, foam-blowing agents and solvents whose atmospheric concentrations are rapidly increasing (O'Doherty et al., 2004; Derwent et al., 2007; Montzka et al., 2009). Their mixing ratios over the oil sands were greater than at any other time during the flight, with maximum values of 212 pptv (HCFC-22) and 22 pptv (HCFC-142b) – or respective enhancements of 12 and 18% over the average background (Table 1; Fig. 8a) – showing their usage and release at the mining sites.

The short-lived solvents $CHCl_3$, C_2HCl_3, C_2Cl_4 and CH_2Cl_2 showed stronger enhancements over the oil sands than during any other portion of the flight (Figs. 4b and 8b), and the maximum C_2HCl_3 and C_2Cl_4 levels (4.8 pptv and 5.9 pptv, respectively; Table 1) were greater in the oil sands plumes than at any other time during the summer phase of ARCTAS. For perspective, these plume values are smaller than average levels measured in urban centers such as Hong Kong, where C_2HCl_3 and C_2Cl_4 mixing ratios of 70±31 and 29±9 pptv were measured during autumn 2007 (Zhang et al., 2010). Maximum respective CH_2Cl_2 and $CHCl_3$ mixing ratios were 35.1 pptv and 15.6 pptv, or 22% and 45% larger than the background average. Methylene chloride, C_2Cl_4, and to a lesser extent $CHCl_3$ were also enhanced relative to background mixing ratios during the descent into Cold Lake, showing their use as solvents in local urban areas as well as by the mining industry.

3.3.2 Minimally enhanced halocarbons

The second group of compounds, which were minimally enhanced over the oil sands, includes 1,1,1,2-tetrafluoroethane (HFC-134a), some chlorinated species (1,2-dichloroethane, HCFC-141b), the halons (H-1211, H-1301, H-2402), and the methyl halides (CH_3Br, CH_3I, CH_3Cl).

HFC-134a is a CFC-12 replacement that is rapidly increasing in the atmosphere (O'Doherty et al., 2004; Clerbaux and Cunnold, 2007), reaching up to 60 pptv in US pollution plumes (Barletta et al., 2009) compared to up to 48.9 pptv in the oil sands plumes (8% larger than the background average), suggesting that the oil sands mining industry is a relatively minor HFC-134a source (Table 1, Fig. 8c). 1,2-Dichloroethane is used as a chemical intermediate and solvent and its maximum mixing ratio over the oil sands (9.4 pptv) was 16% higher than the background BL average but within the range of mixing ratios measured at other times during the flight, also suggesting relatively small emissions by the oil sands industry (Table 1). Likewise, the CFC replacement compound HCFC-141b showed fairly small (<7%) enhancements over the oil sands (Table 1). The halons are ozone-depleting substances that are still used in North America because of their critical role as fire extinguishing agents (Butler et al., 1998; Fraser et al., 1999; Montzka et al., 2003). Maximum H-1211, H-1301 and H-2402 levels over the oil sands were 5–10% greater than the local background average (Table 1), compared to average H-1211 exceedances of 75% in cities in China (Barletta et al., 2006) where 90% of global H-1211 production occurs (Fraser et al., 1999). Therefore the halon enhancements over the oil sands also appear to be relatively minor, though we note that the H-1301 maximum was larger than at any other time during the summer phase of ARCTAS.

Methyl bromide, an ozone-depleting substance with natural and anthropogenic sources (e.g., oceans, salt marshes, fumigation, biomass burning; Yvon-Lewis et al., 2009 and references therein), had a maximum mixing ratio of 8.3 pptv both over the oil sands and upon final descent into Cold Lake. This 8% enhancement over the local background average was small compared to CH_3Br mixing ratios of up to 15 pptv measured in fresh fire plumes during ARCTAS. Methyl iodide is a very short-lived species (1–2 d) that is mainly emitted from the ocean (Yokouchi et al., 2008). Its mixing ratio declined sharply with altitude, consistent with its short atmospheric lifetime (Fig. 8d). Because the mixing ratios of CH_3I during Legs 7 and 9 (<0.45 pptv) are at the low end of global background values (0.5–2 pptv; Yokouchi et al., 2008 and references therein) and because CH_3I did not correlate with other species ($r^2 \leq 0.37$), the oil sands do not appear to be a significant CH_3I source, if at all.

Methyl chloride is the most abundant chlorine-containing compound in the atmosphere. It has a complex budget with multiple sources (e.g., tropical vegetation, biomass burning) and sinks (e.g., OH, soil) (Clerbaux and Cunnold, 2007). During the first half of the flight the average CH_3Cl mixing ratio in the FT was 530±13 pptv, then it decreased to 503±6 pptv in the background BL, consistent with CH_3Cl removal at low altitude by its soil sink. By contrast, the average CH_3Cl mixing ratio over the oil sands (522±12 pptv) was enhanced compared to the local background, with a maximum of 545 pptv and a range of values similar to the FT (Fig. 8e). Whereas CH_3Cl showed poor correlation with most compounds over the oil sands ($r^2 < 0.34$), including combustion tracers such as CO and ethyne ($r^2 < 0.01$), it showed some correlation with OCS and HCFC-22 ($r^2 = 0.58$ for both) followed by HCFC-142b and HFC-134a ($0.46 \leq r^2 \leq 0.47$). Carbonyl sulphide has a strong vegetative sink (Sect. 3.4) and Montzka et al. (2007) found some correlation between OCS and other species with known surface sinks such as CH_3Cl. Therefore the CH_3Cl enhancement is expected to be related to the loss of its soil sink at the mining site, with the possibility of its co-emission from the oil sands industry together with species such as HCFC-22.

3.3.3 Non-enhanced halocarbons

Carbon tetrachloride (CCl_4), methyl chloroform (CH_3CCl_3), and chlorofluorocarbons (CFC-11, CFC-12, CFC-113, and CFC-114) were not statistically enhanced over the oil sands (Table 1; Fig. 4a). These long-lived compounds have been banned in developed countries since 1996 under the Montreal Protocol, and even though evidence exists for their continued emissions in North America (Millet and Goldstein, 2004; Hurst et al., 2006) their absence from the oil sands mining industry is not surprising. Ethyl chloride (C_2H_5Cl), another chlorinated hydrocarbon whose industrial demand is declining, also was not enhanced over the oil sands. Likewise, with the exception of methyl bromide (CH_3Br), none of the measured brominated species ($CHBr_3$, CH_2Br_2, $CHBrCl_2$, $CHBr_2Cl$) were enhanced over the oil sands (Table 1). These short-lived species are predominantly emitted from the ocean (e.g., Butler et al., 2007) and their lack of enhancement over the oil sands is not unexpected.

3.4 Sulphur species

Sulphur dioxide (SO_2) is strongly associated with fossil fuel combustion, especially coal and residential oil, and the sulphur content of crude petroleum can be up to 2% (Benkovitz et al., 1996). In the Athabasca oil sands developments, the major SO_2 emission sources are associated with the upgrading and energy production operations at the Suncor and Syncrude sites (Kindzierski and Ranganathan, 2006; D. Spink, personal communication, 2010). For example Suncor produces high sulphur fuel grade petroleum coke from oil sands at its Fort McMurray operations that is 5.7–6.8% sulphur on a dry basis (http://www.suncor.com/en/about/3408.aspx). Some of this coke is used to power its upgrading operations, emitting SO_2 into the atmosphere as a by-product, but most of the coke is buried as a waste product. Whereas Burstyn et al. (2007)

measured monthly average SO_2 mixing ratios of 300–1300 pptv in rural locations of western Canada, and Kindzierski and Ranganathan (2006) measured a median outdoor SO_2 mixing ratio of 650 pptv in residential areas of Fort McKay (a small community 64 km north of Fort McMurray, in proximity to the mining operations), SO_2 levels in this study were even lower during most of the flight, averaging 17±5 pptv in the FT during the first half of the flight and increasing to 102±27 pptv upon descent into the background BL air (Table 1; Fig. 4d). However, SO_2 showed remarkable enhancements over the oil sands, with a maximum mixing ratio of 38 730 pptv (38.73 ppbv) in sample 4, or 383 times the background BL average. This value is similar to those measured in the urban/industrial environments of heavily polluted cities. For example, Talbot et al. (2008) reported peak airborne SO_2 mixing ratios in excess of 34 000 pptv (34 ppbv) in BL air sampled over Mexico City during the spring 2006 INTEX-B experiment. Similarly de Foy et al. (2009) measured ground-based SO_2 values exceeding 80 000 pptv (80 ppbv) in the Mexico City Metropolitan Area during spring 2006, which they attributed to coal combustion, refineries, and active volcanoes. Here we attribute the elevated SO_2 levels to coke combustion, and the very strong correlations between SO_2 and more than a dozen compounds ($r^2 \geq 0.9$) – most notably the trimethylbenzenes ($0.98 \leq r^2 \leq 0.99$), NO, NO_2 and NO_y ($0.96 \leq r^2 \leq 0.97$), the ethyltoluenes ($0.90 \leq r^2 \leq 0.97$), and ethene ($r^2 = 0.92$) – suggest that coke combustion may be associated with their enhancements as well.

Carbonyl sulphide (OCS) is the most abundant sulphur-containing compound in the remote atmosphere (Ko et al., 2003 and references therein). Its sources include CS_2 oxidation, the oceans, biomass burning, coal burning and aluminum production (e.g., Watts, 2000; Kettle et al., 2002). Like CH_3Cl, the average OCS mixing ratio was fairly constant in the FT during the first half of the flight (445±19 pptv), then diminished with decreasing altitude to 413±13 pptv in background BL air, consistent with its well-known uptake by vegetation (e.g., Montzka et al., 2007; Blake et al., 2008; Campbell et al., 2008). By contrast OCS was not depleted over the oil sands, where its average mixing ratio (437±26 pptv) was not significantly different than during the first half the flight

(Table 1; Fig. 8f). Carbonyl sulphide did not correlate with most compounds over the oil sands ($r^2 \leq 0.38$) but showed some correlation with the same suite of compounds as CH_3Cl, including HCFC-22, HCFC-142b and HFC-134a ($0.47 \leq r^2 \leq 0.58$). Therefore the relative OCS enhancement over the oil sands compared to the background BL is most likely due to a lack of drawdown from the cleared land in the oil sands area, with the possibility of an OCS source associated with the oil sands industry. Note that even though previous work has shown similarities between OCS and CO_2 because of simultaneous uptake by photosynthetically active vegetation (Montzka et al., 2007; Campbell et al., 2008), here OCS and CO_2 showed poor correlation ($r^2=0.16$) because CO_2 has a clear additional fossil fuel source at the oil sands developments (Sect. 3.6).

Dimethyl sulphide (DMS) is a short-lived sulphur species (1–2 days) with a major oceanic source and minor sources including vegetation and biomass burning (Watts et al., 2000; Gondwe et al., 2003; Meinardi et al., 2003). Like CH_3I, DMS strongly decreased with altitude and DMS levels were below detection (< 1 pptv) in the FT, increasing to 4.7±0.8 pptv in the background BL. Its average mixing ratio doubled to 10.7±3.9 pptv over the oil sands, with a maximum enhancement of 18 pptv (Table 1). For comparison, DMS levels over productive oceanic regions are on the order of 100–250 pptv (e.g., Nowak et al., 2001). DMS was most strongly enhanced in samples 4, 5 and 6 and correlated with a range of compounds, most strongly CO_2 ($r^2=0.82$) as well as H-1211, 1,2-dichloroethane and HCFC-142b ($0.71 \leq r^2 \leq 0.74$), indicating that its source is industrial.

3.5 NO, NO_2, NO_y and O_3

Like SO_2, the major source of nitrogen oxides (NO_x) is fossil fuel combustion (Benkovitz et al., 1996). Nitric oxide, NO_2 and NO_y were all very strongly enhanced over the oil sands compared to their respective background values of 16±6, 24±11 and 194±33 pptv (Table 1). The maximum NO, NO_2 and NO_y mixing ratios occurred in sample 4 and were 4980, 4995 and 10 555 pptv, respectively, representing enhancements of 319, 210 and 54 times the local background (Table 1; Fig. 9a and b). (Recall that these numbers are based on the average of those NO, NO_2 and NO_y measurements which overlapped the VOC sampling times (Sect. 3). The maximum NO, NO_2 and NO_y values over the oil sands based on 1 s measurements were even higher: 9545, 9205 and 21 800 pptv, respectively.) The NO maximum was the highest recorded throughout the summer phase of ARCTAS, showing the very strong emissions of nitrogen oxides from the mining industry. The NO_y levels in the oil sands plumes lie within the lower range of values measured in megacities such as Tokyo, Mexico City and Beijing, which can vary from 2000–200 000 pptv (Parrish et al., 2009). The major NO_x sources at the mining sites are (1) the upgraders, gaseous fuel fired boilers, heaters, and co-generation units for heat and power production, and (2) the heavy hauler mine fleets (D. Spink, personal communication, 2010). Because NO, NO_2 and NO_y correlated perfectly with each other (r^2=1.00) and very strongly with SO_2, most C_2–C_4 alkenes, and the C_9 aromatics ($0.90 \leq r^2 \leq 0.99$) (Table 3), we conclude that the observed NO_x emissions were from the upgraders, etc. rather than the heavy hauler fleet.

Ozone was not enhanced over the oil sands, and its maximum mixing ratio (31 ppbv) was the same as the average background BL value (31±1 ppbv) (Table 1, Fig. 9c). In fact O_3 was anti-correlated with NO over the oil sands (Fig. 10) as the very strong NO emissions reacted away some of the O_3, a process which dominated over O_3 production on this short time-scale. Note that in Fig. 10 virtually all (~95%) of the NO_y is in the form of NO_x.

3.6 CO_2, CH_4 and CO

Carbon dioxide (CO_2) is the leading contributor to the enhanced radiative forcing of the atmosphere, followed by methane (CH_4) (Forster et al., 2007). Compared to the FT, CO_2 was relatively depleted in the background BL air during Flight 23 (Table 1, Fig. 9d), consistent with its summertime uptake by terrestrial vegetation (Erickson et al., 1996; Randerson et al., 1997, 1999). By contrast CO_2 showed a clear enhancement over the oil sands, with a maximum mixing ratio of 389 ppmv that is outside the range of values measured during the rest of the flight. Δ^{14}C in CO_2 was depleted in these enhanced samples, indicating a fossil fuel CO_2 influence (not shown). Carbon dioxide correlated with a wide range of compounds associated with the mining industry, including DMS, combustion tracers such as *i*-butene, ethene, ethyne and NO_y, and industrial tracers such as MEK, 2,3-dimethylbutane, $CHCl_3$, and 3-ethyltoluene ($0.72 \le r^2 \le 0.82$), showing its emissions during many stages of the mining operations.

Methane is long-lived and well-mixed in the remote atmosphere, and its sources include biogenic sources (e.g., wetlands, ruminants, rice agriculture), biomass burning, and fossil fuel mining and burning (Denman et al., 2007). Its mixing ratio varied little in the FT during Flight 23, averaging 1836±10 ppbv (Table 1; Fig. 9e). Unfortunately CH_4 measurements were not available during the background BL run (Leg 9). Methane shows a characteristic north-south gradient (e.g., Simpson et al., 2002), and because Cold Lake is at a similar latitude to Leg 9 and does not appear to have been appreciably impacted by local CH_4 sources (Fig. 9e), the average CH_4 mixing ratio in the BL during the final descent into Cold Lake (1843±5 ppbv) is expected to be a reasonable proxy for the local background at this time of year. Methane mixing ratios were clearly enhanced over the oil sands, reaching 1983 ppbv in sample 6. By comparison the maximum CH_4 mixing ratio during the summer phase of ARCTAS was 2000 ppbv in a fresh fire plume sampled on 4 July during Flight 19. Natural gas is heavily used by the oil sands mining industry (Sect. 1), but the CH_4 results are surprising in that CH_4 did not correlate particularly well with ethane and propane ($0.52 \le r^2 \le 0.57$), which, like CH_4, are components of natural gas (the CH_4 composition of commercial-grade natural gas is 70–95%, with the remainder primarily ethane and propane; e.g., McTaggart-Cowan et al., 2010). Methane also did not correlate well with combustion tracers such as CO ($r^2=0.29$) or NO ($r^2=0.37$), and unexpectedly its best correlations were with the industrial and combustion tracers 1-butene ($r^2=0.84$) and *trans*-2-butene ($r^2=0.72$). Although there is a clear CH_4 source from the oil sands, methane's comparatively low correlations with ethane and propane suggest low natural gas leakage levels from the mining operations (Sect. 3.2.1).

Carbon monoxide (CO) is a potentially toxic gas that is also a precursor to photochemical smog. The maximum CO mixing ratio over the oil sands (144 ppbv in sample 5, or 48% greater than the local background of 97±1 ppbv) was comparable to mixing ratios measured at other times during the flight (Table 1; Fig. 9f) and is not considered a large enhancement. For example Baker et al. (2008) found typical summertime CO mixing ratios of 300±66 ppbv in US cities, and CO mixing ratios measured near fresh biomass burning plumes during ARCTAS exceeded 1900 ppbv (not shown). Interestingly, CO correlated most strongly with the suite of C_4–C_9 alkanes, C_6–C_8 aromatics and C_5–C_6 cycloalkanes ($0.85 \leq r^2 \leq 0.97$) that were associated with direct emissions from the oil sands and/or diluent (Sect. 3.2). It also showed good correlations with $CHCl_3$ ($r^2=0.84$) and the C_9 aromatics ($0.66<r^2<0.83$). Carbon monoxide is an urban/industrial combustion tracer and these results suggest that relatively low levels of CO are emitted throughout the mining operations.

4 Conclusions

Mixing ratios of 84 trace gases were measured in boundary layer air over oil sands surface mining operations in northern Alberta on 10 July 2008, aboard the NASA DC-8 research aircraft as part of the 2008 ARCTAS mission. Compared to local background air, 15 of these compounds showed no statistical enhancements over the oil sands (propyne, MTBE, furan, CFC-11, CFC-12, CFC-113, CFC-114, CCl_4, CH_3CCl_3, ethyl chloride, $CHBr_3$, CH_2Br_2, $CHBrCl_2$, $CHBr_2Cl$ and O_3). As is to be expected with high NO levels, O_3 was anti-correlated with NO and it appears that depletion of O_3 by NO dominated over O_3 production on this short time-scale. Another 9 compounds showed minimal enhancements over the oil sands (HFC-134a, HCFC-141b, 1,2-dichloroethane, H-1211, H-1301, H-2402, CH_3Br, CH_3I, CH_3Cl).

The remaining 60 compounds showed greater mixing ratios over the oil sands than at any other time during the flight, or, in the case of CO, it showed a clear (up to 48%) enhancement and strong correlations with many other compounds. The maximum enhancements were 1.1–397 times the background BL values, most notably *n*-heptane

(397×), SO_2 (382×), NO (319×), *n*-octane (242×) and methylcyclohexane (113×). Based on their mutual correlations, the elevated trace gases fell into two groups. The first group included CO and species associated with direct evaporative emissions from the oil sands themselves and/or from the diluent used to lower the viscosity of the recovered bitumen (C_4–C_9 alkanes, C_5–C_6 cycloalkanes, C_6–C_8 aromatics). By contrast to the *n*-alkanes, the enhancements of aromatics such as benzene were relatively low, especially compared to values that have been measured downstream at petrochemical refineries. The CO enhancements were also generally small suggesting that the upgraders emit low levels of CO, which is to be expected for high temperature combustion where the carbon is converted mostly to CO_2 (i.e., efficient combustion). The second group includes a wide variety of species associated with emissions from the mining effort, for example coke combustion (e.g., SO_2) and upgrading (e.g., NO, NO_2, NO_y). The maximum SO_2 and NO levels over the oil sands were higher than at any other time during the summer phase of ARCTAS, and even though northern Alberta is a rural environment the SO_2 and NO_y levels were comparable to those measured in the world‘s megacities. Although the oil sands industry is a major user of natural gas, a strong natural gas signal was not evident in the data, suggesting low natural gas leakage levels and high efficiency combustion associated with the upgraders. Carbon monoxide and the butanes fell into both groups and appear to have multiple sources from oil sands mining.

Isoprene, a biogenic tracer, was enhanced during the oil sands boundary layer run but with a maximum over a vegetated area south of the major mining operations. By contrast, the monoterpenes (also biogenic tracers) were most enhanced in the oil sands plumes and showed good correlations with many industrial species associated with the mining effort, including C_2Cl_4 and SO_2. The possibility of pinene emissions directly associated with the mining operations requires further study. Carbonyl sulphide and CH_3Cl were also notable in that they failed to be drawn down over the surface mining sites, most likely because of the removal of their vegetation and soil sinks, respectively.

These measurements represent the only independent characterization of trace gas emissions from oil sands mining operations of which we are aware. Although the absolute mixing ratios of many VOCs were relatively modest compared to major petrochemical facilities that have been studied, they are significantly enhanced above background levels. The high reactivity of most of these gases, combined with significant emissions of nitrogen oxides and SO_2 in what would otherwise be a relatively pristine area, mean that they do have the potential to form O_3 and acid conditions downwind of this activity. Further study of such potential effects is required, for example modeling and a multi-day ground-based grid study near the mining sites would help to more completely characterize the trace gases that are emitted from and impacted by the Alberta oil sands industry.

Acknowledgements. We thank the ARCTAS crew and science team for their hard work throughout the mission, and we gratefully acknowledge helpful discussions with many of our colleagues, especially Jim Crawford (NASA Langley) and Joost de Gouw (NOAA ESRL). We also thank Michael Petryk (DRDC Suffield) for programming the correlation matrices, and David Spink (Fort McKay IRC) for many helpful comments on the manuscript. This research was funded by NASA grant NNX09AB22G.

References

Alboudwarej, H., Felix, J., Taylor, S., et al.: Highlighting heavy oil, Oilfield Rev., 34–53, 2006.

Apel, E. C., Calvert, J. G., Gilpin, T. M., Fehsenfeld, F. C., Parrish, D. D., and Lonneman, W. A.: The Nonmethane Hydrocarbon Intercomparison Experiment (NOMHICE): task 3, J. Geophys. Res., 104, 21, 26069–26086, 1999.

Apel, E. C., Calvert, J. G., Gilpin, T. M., Fehsenfeld, F., and Lonneman, W. A.: Nonmethane Hydrocarbon Intercomparison Experiment (NOMHICE): Task 4, ambient air, J. Geophys. Res., 108(D9), 4300, doi:10.1029/2002JD002936, 2003.

Atkinson, R.: Gas-phase tropospheric chemistry of organic compounds, J. Phys. Chem. Ref. Data, Monograph, 2, 1–216, 1994.

Atkinson, R.: Atmospheric chemistry of VOCs and NO_x, Atmos. Environ., 34, 2063–2101, 2000.

Atkinson, R. and Arey, J.: Atmospheric degradation of volatile organic compounds, Chem. Rev., 103, 4605–4638, 2003.

Baker, A. K., Beyersdorf, A. J., Doezema, L. A., et al.: Measurements of nonmethane hydrocarbons in 28 United States cities, Atmos. Environ. 42, 170–182, 2008.

Barletta, B., Meinardi, S., Simpson, I. J., et al.: Mixing ratios of volatile organic compounds (VOCs) in the atmosphere of Karachi, Pakistan, Atmos. Environ. 36, 3429–3443, 2002.

Barletta, B., Meinardi, S., Simpson, I. J., Atlas, E. L., Beyersdorf, A. J., Baker, A. K., Blake, N. J., Yang, M., Midyett, J. R., Novak, B. J., McKeachie, R. J., Fuelberg, H. E., Sachse, G. W., Avery, M. A., Campos, T., Weinheimer, A. J., Rowland, F. S., and Blake, D. R.: Characterization of volatile organic compounds (VOCs) in Asian and north American pollution plumes during INTEX-B: identification of specific Chinese air mass tracers, Atmos. Chem. Phys., 9, 5371–5388, doi:10.5194/acp-9-5371-2009, 2009.

Barletta, B., Meinardi, S., Rowland, F. S., et al.: Volatile organic compounds in 43 Chinese cities, Atmos. Environ., 39 5979–5990, 2005.

Benkovitz, C. M., Scholtz, M. T., Pacyna, J., et al.: Global gridded inventories of anthropogenic emissions of sulphur and nitrogen, J. Geophys. Res., 101(D22), doi:10.1029/96JD00126, 1996.

Blake, D. R. and Rowland, F. S.: Continuing world-wide increase in tropospheric methane, 1978–1987, Science, 239, 1129–1131, 1988.

Blake, D. R. and Rowland, F. S.: Urban leakage of liquefied petroleum gas and its impacts on Mexico City air quality, Science, 269, 953–956, 1995.

Blake, N. J., Blake, D. R., Sive, B. C., et al.: Biomass burning emissions and vertical distribution of atmospheric methyl halides and other reduced carbon gases in the South Atlantic region, J. Geophys. Res., 101(D19), 24151–24164, 1996.

Blake, N. J., Blake, D. R., Simpson, I. J., et al.: NMHCs and halocarbons in Asian continental outflow during the transport and chemical evolution over the Pacific (TRACE-P) field campaign: Comparison with PEM-West B, J. Geophys. Res., 108(D20), 8806, doi:/10.1029/2002JD003367, 2003.

Blake, N. J., Campbell, J. E., Vay, S. A., et al.: Carbonyl sulfide (OCS): Large-scale distributions over North America during INTEX-NA and relationship to CO_2, J. Geophys. Res., 113, D09S90, doi:10.1029/2007JD009163, 2008.

Borbon, A., Fontaine, H., Veillerot, M., et al.: An investigation into the traffic-related fraction of isoprene at an urban location, Atmos. Environ., 35, 3749–3760, 2001.

Burstyn, I., Senthilselvan, A., Kim, H.-M., Cherry, N. M., Pietroniro, E., and Waldner, C.: Industrial sources influence air concentrations of hydrogen sulfide and sulfur dioxide in rural areas of western Canada, J. Air Waste Manage., 57(10), 1241–1250, 2007.

Butler, J. H., Montzka, S. A., Clarke, A. D., Lobert, J. M., and Elkins, J. W.: Growth and distribution of halons in the atmosphere, J. Geophys. Res., 103(D1), 1503–1511, 1998.

Butler, J. H., King, D. B., Lobert, J. M., et al.: Oceanic distributions and emissions of short-lived halocarbons, Global Biogeochem. Cy., 21, GB1023, doi:10.1029/2006GB002732, 2007.

Buzcu, B. and Fraser, M. P.: Source identification and apportionment of volatile organic compounds in Houston, TX, Atmos. Environ., 40, 2385–2400, 2006.

Campbell, J. E., Carmichael, G. R., Chai, T., Mena-Carrasco, M., Tang, Y., Blake, D. R., Blake, N. J., Vay, S. A., Collatz, G. J., Baker, I., Berry, J. A., Montzka, S. A., Sweeney, C., Schnoor, J. L., and Stanier, C. O.: Photosynthetic control of atmospheric carbonyl sulfide during the growing season, Science, 322, 1085–1088, 2008.

Choi, Y., Elliott, S., Simpson, I. J., et al.: Survey of whole air data from the second airborne biomass burning and lightning experiment using principal component analysis, J. Geophys. Res., 108(D5), doi:10.1029/2002JD002841, 2003.

Colman, J. J., Swanson, A. L., Meinardi, S., Sive, B. C., Blake, D. R., and Rowland, F. S.: Description of the analysis of a wide range of volatile organic compounds in whole air samples collected during PEM-Tropics A and B, Anal. Chem., 73, 3723–3731, 2001.

Clerbaux, C., Cunnold, D. M., Anderson, J., et al.: Long-lived compounds, Scientific Assessment of Ozone Depletion: 2006 Global Ozone Research and Monitoring Project, Report no. 50, Chapter 1, World Meteorological Organization, Geneva, 2007.

de Foy, B., Krotkov, N. A., Bei, N., Herndon, S. C., Huey, L. G., Martínez, A.-P., Ruiz-Suárez, L. G., Wood, E. C., Zavala, M., and Molina, L. T.: Hit from both sides: tracking industrial and volcanic plumes in Mexico City with surface measurements and OMI SO_2 retrievals during the MILAGRO field campaign, Atmos. Chem. Phys., 9, 9599–9617, doi:10.5194/acp-9-9599-2009, 2009.

De Gouw, J. A., Te Lintel Hekkert, S., Mellqvist, J., et al.: Airborne measurements of ethene from industrial sources using Laser Photo-Acoustic Spectroscopy, Environ. Sci. Technol., 43, 7, 2437–2442, 2009.

Denman, K. L., Brasseur, G., Chidthaisong, A., et al.: Couplings between changes in the climate system and biogeochemistry, In: Climate Change 2007: The Physical Science Basis. Contribution of Working Group I to the Fourth Assessment Report of the Intergovernmental Panel on Climate Change, edited by: Solomon, S., Qin, D., Manning, M., Chen, Z., Marquis, M., Averyt, K. B., Tignor, M., and Miller, H. L., Cambridge University Press, Cambridge, UK and New York, NY, USA, 2007.

Derwent, R. G., Simmonds, P. G., Greally, B. R., et al.: The phase-in and phase-out of European emissions of HCFC-141b and HCFC-142b under the Montreal Protocol: Evidence from observations at Mace Head, Ireland and Jungfraujoch, Switzerland from 1994 to 2004, Atmos. Environ., 41, 757–767, 2007.

Ehhalt, D. H. and Prather, M.: Atmospheric chemistry and greenhouse gases, in: Climate Change 2001: The Scientific Basis, Cambridge Univ. Press, New York, 245–287, 2001.

Erickson, D. J., Rasch, P. J., Tans, P. P., et al.: The seasonal cycle of atmospheric CO_2: A study based on the NCAR Community Climate Model (CCM2), J. Geophys. Res., 101, 15079–15097, 1996.

Folberth, G. A., Hauglustaine, D. A., Lathère, J., and Brocheton, F.: Interactive chemistry in the Laboratoire de Météorologie Dynamique general circulation model: model description and impact analysis of biogenic hydrocarbons on tropospheric chemistry, Atmos. Chem. Phys., 6, 2273–2319, doi:10.5194/acp-6-2273-2006, 2006.

Forster, P., Ramaswamy, V., Artaxo, P., et al.: Changes in Atmospheric Constituents and in Radiative Forcing. In: Climate Change 2007: The Physical Science Basis. Contribution of Working Group I to the Fourth Assessment Report of the Intergovernmental Panel on Climate Change, edited by: Solomon, S., Qin, D., Manning, M., Chen, Z., Marquis, M., Averyt, K. B., Tignor, M., and Miller, H. L., Cambridge University Press, Cambridge, UK and New York, NY, USA, 2007.

Fraser, P. J., Oram, D. E., Reeves, C. E., Penkett, S. A., and McCulloch, A.: Southern hemispheric halon trends (1978–1998) and global halon emissions, J. Geophys. Res., 104(D13), 15985–16000, 1999.

Fried, A., Diskin, G., Weibring, P., et al.: Tunable infrared laser instruments for airborne atmospheric studies, Appl. Phys. B, 92(3), 409–417, 2008.

Fuelberg, H. E., Harrigan, D. L., and Sessions, W.: A meteorological overview of the ARCTAS 2008 mission, Atmos. Chem. Phys., 10, 817–842, doi:10.5194/acp-10-817-2010, 2010.

Fuentes, J. D., Lerdau, M., Atkinson, R., et al.: Biogenic hydrocarbons in the atmospheric boundary layer: A review, B. Am. Meteorol. Soc., 81(7), 1537–1575, 2000.

Gilman, J. B., Kuster, W. C., Goldan, P. D., et al.: Measurements of volatile organic compounds during the 2006 TexAQS/GoMACCS campaign: Industrial influences, regional characteristics, and diurnal dependencies of the OH reactivity, J. Geophys. Res., 114, D00F06, doi:10.1029/2008JD011525, 2009.

Gondwe, M., Krol, M., Gieskes, W., Klaassen, W., and de Baar, H.: The contribution of ocean-leaving DMS to the global atmospheric burdens of DMS, MSA, SO_2, and NSS SO_4^{2-}, Global Biogeochem. Cy., 17(2), 1056, doi:10.1029/2002GB001937, 2003.

Guenther, A., Geron, C., Pierce, T., Lamb, B., Harley, P., and Fall, R.: Natural emissions of non-methane volatile organic compounds, carbon monoxide, and oxides of nitrogen from North America, Atmos. Environ., 34, 2205–2230, 2000.

Guenther, A., Karl, T., Harley, P., Wiedinmyer, C., Palmer, P. I., and Geron, C.: Estimates of global terrestrial isoprene emissions using MEGAN (Model of Emissions of Gases and Aerosols from Nature), Atmos. Chem. Phys., 6, 3181–3210, doi:10.5194/acp-6-3181-2006, 2006.

Horowitz, L. W., Walters, S., Mauzerall, D. L., et al.: A global simulation of tropospheric ozone and related tracers: Description and evaluation of MOZART, version 2, J. Geophys. Res., 108 (D24), 4784, doi:10.1029/2002JD002853, 2003.

Hurst, D. F., Lin, J. C., Romashkin, P. A., et al.: Continuing global significance of emissions of Montreal Protocol-restricted halocarbons in the USA and Canada, J. Geophys. Res., 111, D15302, doi:10.1029/2005JD006785, 2006.

Jacob, D. J., Field, B. D., Li, Q. et al.: Global budget of methanol: Constraints from atmospheric observations, J. Geophys. Res., 110, D08303, doi:10.1029/2004JD005172, 2005.

Jacob, D. J., Crawford, J. H., Maring, H., Clarke, A. D., Dibb, J. E., Emmons, L. K., Ferrare, R. A., Hostetler, C. A., Russell, P. B., Singh, H. B., Thompson, A. M., Shaw, G. E., McCauley, E., Pederson, J. R., and Fisher, J. A.: The Arctic Research of the Composition of the Troposphere from Aircraft and Satellites (ARCTAS) mission: design, execution, and first results, Atmos. Chem. Phys., 10, 5191–5212, doi:10.5194/acp-10-5191-2010, 2010.

Karl, T., Apel, E., Hodzic, A., Riemer, D. D., Blake, D. R., and Wiedinmyer, C.: Emissions of volatile organic compounds inferred from airborne flux measurements over a megacity, Atmos. Chem. Phys., 9, 271–285, doi:10.5194/acp-9-271-2009, 2009.

Karl, T., Guenther, A., Turnipseed, A., Tyndall, G., Artaxo, P., and Martin, S.: Rapid formation of isoprene photo-oxidation products observed in Amazonia, Atmos. Chem. Phys., 9, 7753–7767, doi:10.5194/acp-9-7753-2009, 2009.

Katzenstein, A. S., Doezema, L. A., Simpson, I. J., Blake, D. R., and Rowland, F. S.: Extensive regional atmospheric hydrocarbon pollution in the Southwestern United States, Proc. Nat. Acad. Sc., 100, 11975–11979, 2003.

Kettle, A. J., Kuhn, U., von Hobe, M., Kesselmeier, J., and Andreae, M. O.: Global budget of atmospheric carbonyl sulfide: temporal and spatial variations of the dominant sources and sinks, J. Geophys. Res., 107(D22), 4658, doi:10.1029/2002JD002187, 2002.

Kim, S., Huey, L. G., Stickel, R. E., et al.: Measurement of HO_2NO_2 in the free troposphere during the Intercontinental Chemical Transport Experiment-North America 2004, J. Geophys. Res., 112, doi:10.1029/2006JD007676, 2007.

Kindzierski, W. B. and Ranganathan, H. K. S.: Indoor and outdoor SO_2 in a community near oil sand extraction and production facilities in Northern Alberta, J. Environ. Eng. Sci., 5, S121–S129, 2006.

Ko, M. K. W., Poulet, G., Blake, D., et al.: Very short-lived halogen and sulfur substances, Scientific Assessment of Ozone Depletion: 2002 Global Ozone Research and Monitoring Project, Report no. 47, Chapter 2, World Meteorological Organization, Geneva, 2003.

McTaggart-Cowan, G. P., Rogak, S. N., Munshi, S. R., Hill, P. G., and Bushe, W. K.: The influence of fuel composition on a heavy-duty, natural-gas direct-injection engine, Fuel, 89, 752–759, 2010.

Meinardi, S., Simpson, I. J., Blake, N. J., Blake, D. R., and Rowland, F. S.: Dimethyl disulfide (DMDS) and dimethyl sulfide (DMS) emissions from biomass burning in Australia, Geophys. Res. Lett., 30(9), 1454, 10.1029/2003GL016967, 2003.

Millet, D. B. and Goldstein, A. H.: Evidence of continuing methylchloroform emissions from the United States, Geophys. Res. Lett., 31, L17101, doi:10.1029/2004GL020166, 2004.

Mintz, R. and McWhinney, R. D.: Characterization of volatile organic compound emission sources in Fort Saskatchewan, Alberta using principal component analysis, J. Atmos. Chem., 60(1), 83–101, 2008.

Montzka, S. A., Fraser, P. J., Butler, J., et al.: Controlled substances and other source gases, Chapter 1, in Scientific Assessment of Ozone Depletion: 2002, Global Ozone Res. and Monitor. Proj., Vol. No. 47, World Meteorol. Org., Geneva, Switzerland, 2003.

Montzka, S. A., Calvert, P., Hall, B. D., et al.: On the global distribution, seasonality, and budget of atmospheric carbonyl sulfide (COS) and some similarities to CO_2, J. Geophys. Res., 112, D09302, doi:10.1029/2006JD007665, 2007.

Montzka, S. A., Hall, B. D., and Elkins, J. W.: Accelerated increases observed for hydrochlorofluorocarbons since 2004 in the global atmosphere, Geophys. Res. Lett., 36, L03804, doi:10.1029/2008GL036475, 2009.

Nowak, J. B., Davis, D. D., Chen, G., et al.: Airborne observations of DMSO, DMS, and OH at marine tropical latitudes, Geophys. Res. Lett., 28(11) 2201–2204, 2001.

O'Doherty, S., Cunnold, D. M., Manning, A., et al.: Rapid growth of hydrofluorocarbon 134a and hydrochlorofluorocarbons 141b, 142b and 22 from Advanced Global Atmospheric Gases Experiment (AGAGE) observations at Cape Grim, Tasmania, and Mace Head, Ireland, J. Geophys. Res., 109, D06310, doi:10.1029/2003JD004277, 2004.

Paatero, P.: Least squares formation of robust non-negative factor analysis, Chemometr. Intell. Lab., 37, 15–35, 1997.

Parrish, D. D., Kuster, W., C., Shao, M., et al.: Comparison of air pollutant emissions among mega-cities, Atmos. Environ., 43(40), 6435–6441, 2009.

Randerson, J. T., Thompson, M. V., Conway, T. J., Fung, I. Y., and Field, C. B.: The contribution of terrestrial sources and sinks to trends in the seasonal cycle of atmospheric carbon dioxide, Global Biogeochem. Cy., 11, 535–560, 1997.

Randerson, J. T., Field, C. B., Fung, I. Y., and Tans, P. P.: Increases in early season ecosystem uptake explain recent changes in the seasonal cycle of atmospheric at high northern latitudes, Geophys. Res. Lett., 26(17), 2765–2768, 1999.

Ras, M. R., Marcé, R. M., and Borrull, F.: Characterization of ozone precursor volatile organic compounds in urban atmospheres and around the petrochemical industry in the Tarragona region, Sci. Total Environ., 407(14), 4312–4319, 2009.

Reimann, S., Calanca, P., and Hofer, P.: The anthropogenic contribution to isoprene concentrations in a rural atmosphere, Atmos. Environ., 34(1), 109–115, 2000.

Rogers, M. A. and Koons, C. B.: Generation of light hydrocarbons and establishment of normal paraffin preferences in crude oils, Adv. Chem., 103(3), 67–80, 1971.

Ryerson, T. B., Trainer, M., Angevine, W. M., et al.: Effect of petrochemical industrial emissions of reactive alkenes and NO_x on tropospheric ozone formation in Houston, Texas, J. Geophys. Res., 108(D8), 4249, doi:10.1029/2002JD003070, 2003.

Schade, G. W. and Goldstein, A. H.: Increase of monoterpene emissions from a pine plantation as a result of mechanical disturbances, Geophys. Res. Lett., 30(7), 1380, doi:10.1029/2002GL016138, 2003.

Siddique, T., Fedorak, P. M., and Foght, J. M.: Biodegradation of short-chain *n*-alkanes in oil sands tailings under methanogenic conditions, Environ. Sci. Technol., 40, 5459–5464, 2006.

Siddique, T., Fedorak, P. M., MacKinnon, M. D., and Foght, J. M.: Metabolism of BTEX and naphtha compounds to methane in oil sands tailings, Environ. Sci. Technol., 41, 2350–2356, 2007.

Simpson, I. J., Blake, D. R., Rowland, F. S., and Chen, T.-Y.: Implications of the recent fluctuations in the growth rate of tropospheric methane, Geophys. Res. Lett., 29(10), 672–675, 2002.

Simpson, I. J., Wang, T., Guo, H., Kwok, Y. H., Flocke, F., Atlas, E., Meinardi, S., Rowland, F. S., and Blake, D. R.: Long-term amospheric measurements of C_1–C_5 alkyl nitrates in the Pearl River Delta region of Southeast China, Atmos. Environ., 40, 1619–1632, 2006.

Sive, B. C.: Atmospheric nonmethane hydrocarbons: Analytical methods and estimated hydroxyl radical concentrations, Ph.D Thesis, University of California, Irvine, CA, 1998.

Sprengnether, M., Demerjian, K. L., Donahue N. M., and Anderson, J. G.: Product analysis of the OH oxidation of isoprene and 1,3-butadiene in the presence of NO, J. Geophys. Res., 107(D15), 4268, doi:/10.1029/2001JD000716, 2002.

Talbot, R., Mao, H., Scheuer, E., Dibb, J., Avery, M., Browell, E., Sachse, G., Vay, S., Blake, D., Huey, G., and Fuelberg, H.: Factors influencing the large-scale distribution of Hg° in the Mexico City area and over the North Pacific, Atmos. Chem. Phys., 8, 2103–2114, doi:10.5194/acp-8-2103-2008, 2008.

Thurston, G. D. and Spengler, J. D.: A quantitative assessment of source contributions to inhalable particulate matter pollution in metropolitan Boston, Atmos. Environ., 19(1), 9–25, 1985.

Timoney, K. P. and Lee, P.: Does the Alberta tar sands industry pollute? The scientific evidence, Open Conservation Biol. J., 3, 65–81, 2009.

Vay, S. A., Anderson, B. E., Conway, T. J., et al.: Airborne observations of the tropospheric CO_2 distribution and its controlling factors over the South Pacific Basin, J. Geophys. Res., 104(D5), 5663–5676, 1999.

Vay, S. A., Woo, J. H., Anderson, B. E., et al.: The influence of regional-scale anthropogenic emissions on CO_2 distributions over the Western North Pacific, J. Geophys. Res., 108(D20), 8801, doi:10.1029/2002JD003094, 2003.

Warneke, C., McKeen, S. A., de Gouw, J. A., et al.: Determination of urban volatile organic compound emission ratios and comparison with an emissions database, J. Geophys. Res., 112, D10S47, doi:10.1029/2006JD007930, 2007.

Watson, J. G., Chow, J. C., and Fujita, E. M.: Review of volatile organic compound source apportionment by chemical mass balance, Atmos. Environ., 35(9), 1567–1584, 2001.

Watts, S. F.: The mass budgets of carbonyl sulfide, dimethyl sulfide, carbon disulfide and hydrogen sulfide, Atmos. Environ., 34, 761–779, 2000.

Weinheimer, A. J., Walega, J. G., Ridley, B. A., Gary, B. L., Blake, D. R., Blake, N. J., Rowland, F. S., Sachse, G. W., Anderson, B. E., and Collins, J. E.: Meridional distributions of NO_x, NO_y, and other species in the lower stratosphere and upper troposphere during AASE II, Geophys. Res. Lett., 21, 2583–2586, 1994.

White, M. L., Russo, R. S., Zhou, Y., Ambrose, J. L., Haase, K., Frinak, E. K., Varner, R. K., Wingenter, O. W., Mao, H., Talbot, R., and Sive, B. C.: Are biogenic emissions a significant source of summertime atmospheric toluene in the rural Northeastern United States?, Atmos. Chem. Phys., 9, 81–92, doi:10.5194/acp-9-81-2009, 2009.

Yokouchi, Y., Osada, K., Wada, M., et al.: Global distribution and seasonal concentration change of methyl iodide in the atmosphere, J. Geophys. Res., 113, D18311, doi:10.1029/2008JD009861, 2008.

Zhang, Y. L., Guo, H., Wang, X. M., et al.: Emission patterns and spatiotemporal variations of halocarbons in the Pearl River Delta region, Southern China, J. Geophys. Res., doi:10.1029/2009JD013726, in press, 2010.

Table 1. Statistics of boundary layer measurements for 84 compounds measured near oil sands surface mining north of Fort McMurray, Alberta on 10 July 2008 (n=17). Concurrent local background values in the boundary layer ("Bkgd") are also included (n=6), as are free tropospheric measurements ("FT") between 60–76° N (n=66). "Max. Enh."=Maximum enhancement of oil sands over background values (oil sands max/bkgd avg); when the background mixing ratio is below detection limit ("LOD") a mixing ratio of 1.5 pptv is assumed. "n/a"=not applicable. Units: pptv unless otherwise stated.

						Oil sands				BKGD		FT		
Compound	Formula	Lifetime[a]	LOD (pptv)	Precision[b] (%)	Accuracy (%)	Min (pptv)	Max (pptv)	Avg (pptv)	StD (pptv)	Avg (pptv)	StD (pptv)	Avg (pptv)	StD (pptv)	Max. Enh.
Sulphur dioxide	SO_2	1 day	20	12	10	119	38730	4697	11525	102	27	17	5	382
Nitric oxide	NO	10 s	20	2	10	7	4980	635	1403	16	6	3	10	319
Nitrogen dioxide	NO_2	1 day	30	5	10	19	4995	678	19	24	11	8	15	210
Total reactive nitrogen	NO_y	n/a	20	1	10	211	10 555	1620	2888	194	33	424	166	54
Ozone	O_3 (ppbv)	8 day	40	1	5	25	31	28	2	31	0	75	23	0.98
Carbon dioxide	CO_2 (ppmv)	>100 yr	n/a	0.1 ppmv	0.25 ppmv	378	389	381	4	378	1	382	1	1.03
Methane	CH_4 (ppbv)	9 yr	n/a	0.1	2	1844	1983	1876	35	1843[f]	5	1836	10	1.08[f]
Carbon monoxide	CO (ppbv)	2 mo	n/a	1	1	97	144	103	11	97	1	111	13	1.48
Alkanes														
Ethane	C_2H_6	47 day[c]	3	1	5	754	1492	917	174	781	22	813	73	1.9
Propane	C_3H_8	11 day[c]	3	2	5	214	714	382	135	200	26	127	20	3.6
i-Butane	C_4H_{10}	5.5 day[c]	3	3	5	32	290	89	69	29	9	7	4	10
n-Butane	C_4H_{10}	4.9 day[c]	3	3	5	64	765	202	179	63	19	14	7	12
i-Pentane	C_5H_{12}	3.2 day[c]	3	3	5	31	564	141	132	22	10	3	4	26
n-Pentane	C_5H_{12}	3.0 day[c]	3	3	5	27	510	116	119	21	8	LOD	n/a	24
n-Hexane	C_6H_{14}	2.2 day[c]	3	3	5	6	294	44	74	5	3	LOD	n/a	65
n-Heptane	C_7H_{16}	1.7 day[c]	3	3	5	LOD	596	70	158	LOD	n/a	LOD	n/a	397
n-Octane	C_8H_{18}	1.4 day[c]	3	3	5	LOD	363	45	101	LOD	n/a	LOD	n/a	242
n-Nonane	C_9H_{20}	1.2 day[c]	3	3	5	LOD	91	13	25	LOD	n/a	3	3	61
2+3-Methylpentane	C_6H_{14}	2.2 day[c]	3	3	5	11	288	57	71	9	4	LOD	n/a	34
2,3-Dimethylbutane	C_6H_{14}	2.0 day[c]	3	3	5	LOD	28	5	8	LOD	n/a	LOD	n/a	19
Ethene	C_2H_4	1.4 day[c]	3	3	5	23	270	69	69	20	2	4	11	14
Propene	C_3H_6	11 h[c]	3	3	5	7	128	28	30	LOD	n/a	LOD	n/a	85
1-Butene	C_4H_8	8.8 h[c]	3	3	5	LOD	72	13	25	LOD	n/a	LOD	n/a	48
i-Butene	C_4H_8	5.4 h[c]	3	3	5	4	37	9	9	LOD	n/a	LOD	n/a	25
cis-2-Butene	C_4H_8	4.9 h[c]	3	3	5	LOD	9	LOD	n/a	LOD	n/a	LOD	n/a	6
trans-2-Butene	C_4H_8	4.3 h[c]	3	3	5	LOD	18	3	6	LOD	n/a	LOD	n/a	12
1,3-Butadiene	C_4H_6	4.2 h[c]	3	3	5	LOD	8	LOD	n/a	LOD	n/a	LOD	n/a	5
Isoprene	C_5H_8	2.8 h[c]	3	3	5	243	780	468	147	311	95	LOD	n/a	2.5
Alkynes														
Ethyne	C_2H_2	12–17 day	3	3	5	56	138	74	22	59	5	106	34	2.4
Propyne	C_3H_4	2 day	5	30	20	LOD	n/a	LOD	n/a	LOD	n/a	LOD	n/a	n/a
Cycloalkanes														
Cyclopentane	C_5H_{10}	2.3 day[c]	3	3	5	LOD	41	9	10	LOD	n/a	LOD	n/a	27
Methylcyclopentane	C_6H_{12}		3	3	5	4	185	31	47	6	2	3	1	62
Cyclohexane	C_6H_{12}	1.7 day[c]	3	3	5	5	133	23	33	4	1	LOD	n/a	87
Methylcyclohexane	C_7H_{14}	1.3 day[c]	3	3	5	4	339	52	100	3	2	3	2	113
Aromatics														
Benzene	C_6H_6	9.5 day[c]	3	3	5	13	82	24	18	11	1	21	10	7
Toluene	C_7H_8	2.1 day[c]	3	3	5	6	401	50	102	6	1	LOD	n/a	73
Ethylbenzene	C_8H_{10}	1.7 day[c]	3	3	5	LOD	84	8	21	LOD	n/a	LOD	n/a	56
m+*p*-Xylene	C_8H_{10}	12–19 h[c,d]	3	3	5	LOD	272	29	74	LOD	n/a	LOD	n/a	181
o-Xylene	C_8H_{10}	20 h[c]	3	3	5	LOD	127	14	37	LOD	n/a	LOD	n/a	85
n-Propylbenzene	C_9H_{12}	2.0 day[c]	3	3	5	LOD	13	2	4	LOD	n/a	LOD	n/a	9
m-Ethyltoluene	C_9H_{12}	15 h[c]	3	3	5	LOD	27	4	9	LOD	n/a	LOD	n/a	18
o-Ethyltoluene	C_9H_{12}	23 h[c]	3	3	5	LOD	17	2	5	LOD	n/a	LOD	n/a	11
p-Ethyltoluene	C_9H_{12}	24 h[c]	3	3	5	LOD	20	2	6	LOD	n/a	LOD	n/a	13
1,2,3-Trimethylbenzene	C_9H_{12}	8.5 h[c]	3	3	5	LOD	40	5	11	LOD	n/a	LOD	n/a	27
1,2,4-Trimethylbenzene	C_9H_{12}	8.5 h[c]	3	3	5	LOD	51	6	15	LOD	n/a	LOD	n/a	34
1,3,5-Trimethylbenzene	C_9H_{12}	4.9 h[c]	3	3	5	LOD	10	1	3	LOD	n/a	LOD	n/a	7

Table 1. Continued.

						Oil sands				BKGD		FT		
Compound	Formula	Lifetime[a]	LOD (pptv)	Precision[b] (%)	Accuracy (%)	Min (pptv)	Max (pptv)	Avg (pptv)	StD (pptv)	Avg (pptv)	StD (pptv)	Avg (pptv)	StD (pptv)	Max. Enh.
Monoterpenes														
α-Pinene	$C_{10}H_{16}$	5.3 h[c]	3	3	5	15	217	67	52	20	7	LOD	n/a	11
β-Pinene	$C_{10}H_{16}$	3.7 h[c]	3	3	5	38	610	226	149	84	24	LOD	n/a	7
Oxygenantes														
Methanol	CH_3OH	12 day[c]	50	30	20	1848	3570	2515	513	1967	354	2276	816	1.8
Ethanol	C_2H_5OH	3.6 day[c]	20	30	20	76	141	106	23	75	12	81	20	1.9
Acetone	C_3H_6O	68 day[c]	100	30	20	393	941	644	154	519	71	947	229	1.8
MEK	C_4H_8O	9.5 day[c]	5	30	20	20	214	65	49	20	16	57	27	11
MAC	C_4H_6O	9.6 h[c]	5	30	20	26	266	92	63	35	10	3	4	8
MVK	C_4H_6O	14 h[c]	5	30	20	42	379	141	109	64	25	16	10	6
MTBE	$C_5H_{12}O$	3.9 day[c]	1	30	20	LOD	n/a	LOD	n/a	LOD	n/a	LOD	n/a	n/a
Furan	C_4H_4O		10	30	20	LOD	n/a	LOD	n/a	LOD	n/a	LOD	n/a	n/a
Halocarbons														
CFC-11	$CFCl_3$	45 yr[e]	10	1	3	251	254	253	1	252.7	0.8	248.4	2.4	1.01
CFC-12	CF_2Cl_2	100 yr[e]	10	1	3	526	538	534	3.2	532.3	1	529.2	3.2	1.01
CFC-113	CCl_2FCClF_2	85 yr[e]	5	1	3	77.5	79.5	78.6	0.6	78.1	0.5	78.2	0.7	1.02
CFC-114	$CClF_2CClF_2$	300 yr[e]	1	1	10	16.2	16.8	16.5	0.1	16.4	0.2	16	0.2	1.02
Methyl chloroform	CH_3CCl_3	5.0 yr[e]	0.1	1	5	12.1	12.6	12.3	0.2	12.2	0.1	12.2	0.1	1.04
Carbon tetrachloride	CCl_4	26 yr[e]	1	1	5	91.8	93.4	92.7	0.4	92.3	0.3	91.7	0.9	1.01
Halon-1211	$CBrClF_2$	16 yr[e]	0.1	1	5	4.09	4.37	4.22	0.1	4.16	0.05	4.23	0.07	1.05
Halon-1301	$CBrF_3$	65 yr[e]	0.1	10	10	3	3.5	3.3	0.15	3.18	0.12	3.12	0.13	1.1
Halon-2402	$CBrF_2CBrF_2$	20 yr[e]	0.01	1	5	0.51	0.54	0.52	0.01	0.51	0.01	0.51	0.01	1.06
HFC-134a	CH_2FCF_3	14 yr[e]	1	3	10	44	48.9	46.7	1.3	45.3	0.6	46.6	1.6	1.08
HCFC-22	CHF_2Cl	12 yr[e]	2	5	5	189.2	212.1	200	6.7	188.7	1.1	193.4	5.8	1.12
HCFC-141b	CH_3CCl_2F	9.3 yr[e]	0.5	3	10	19.9	21.8	21.2	0.4	20.4	0.7	20.8	0.6	1.07
HCFC-142b	CH_2CClF_2	18 yr[e]	0.5	3	10	18.5	22.1	20.1	1	18.8	0.2	19.5	0.6	1.18
Methyl bromide	CH_3Br	0.7 yr[e]	0.5	5	10	7.6	8.3	8	0.2	7.7	0.1	8.3	0.7	1.08
Methyl chloride	CH_3Cl	1.0 yr[e]	50	5	10	508	545	522	12	503	6	530	13	1.08
Methyl iodide	CH_3I	4 d	0.005	5	20	0.37	0.45	0.41	0.02	0.36	0.01	0.06	0.04	1.26
Methylene bromide	CH_2Br_2	3–4 mo	0.01	5	20	0.76	0.94	0.87	0.04	0.91	0.03	0.75	0.05	1.03
Methylene chloride	CH_2Cl_2	3–5 mo	1	5	10	28.4	35.1	31.3	1.8	28.9	0.6	30.9	1.7	1.22
Chloroform	$CHCl_3$	3–5 mo	0.1	5	10	10.3	15.6	11.7	1.3	10.8	0.3	10.4	0.6	1.45
Trichloroethene	C_2HCl_3		0.01	5	10	0.1	4.8	0.6	1.2	0.1	0	0.1	0	33.8
Tetrachloroethene	C_2Cl_4	2–3 mo	0.01	5	10	2.7	5.9	3.2	0.8	2.8	0.1	2.9	0.3	2.12
1,2-Dichloroethane	$C_2H_4Cl_2$	1–2 mo	0.1	5	10	7.4	9.4	8.5	0.6	8.1	0.5	8.9	0.8	1.16
Bromodichloromethane	$CHBrCl_2$	2–3 mo	0.01	10	50	0.14	0.17	0.15	0.01	0.15	0.01	0.15	0.01	1.12
Dibromochloromethane	$CHBr_2Cl$	2–3 mo	0.01	5	50	0.09	0.13	0.12	0.01	0.13	0.01	0.11	0.02	1.03
Bromoform	$CHBr_3$	11 mo	0.01	10	20	0.7	0.91	0.83	0.05	0.9	0.04	0.47	0.31	1.01
Ethyl chloride	C_2H_5Cl		0.1	5	30	0.75	2.62	1.42	0.47	1.39	0.68	1.67	0.62	1.89
Sulphur Compounds														
Carbonyl sulphide	OCS	2.5 yr	10	2	10	392	484	437	26	413	13	445	19	1.17
Dimethyl sulphide	CH_3SCH_3	1–2 d	1	10	20	6	18	10.7	3.9	4.7	0.8	LOD	n/a	3.9

[a] Lifetimes of short-lived OH-controlled compounds are shorter (longer) during the summer (winter), when there are more (fewer) hydroxyl radicals (OH) available for oxidative reactions.

[b] The VOC precision deteriorates as we approach our detection limit; at low values the precision is either the stated precision (%) or 3 pptv, whichever is larger. The NO, NO_2, NO_y and O_3 precision values are for high mixing ratios as were encountered over the oil sands; at low mixing ratios their precision is 20 pptv for the nitrogen species and 0.1 ppbv for O_3.

[c] Based on OH rate constants from Atkinson and Arey (2003) and assuming a 12-h daytime average OH radical concentration of 2.0×10 molec cm^{-3}.

[d] The OH-lifetimes of *m*-xylene and *p*-xylene are 12.0 and 19.4 h, respectively.

[e] Total lifetimes based on Clerbaux and Cunnold (2007).

[f] CH_4 mixing ratios were not measured during Leg 9, and the background value was determined from the Cold Lake landing (see text).

Table 2. Mixing ratios of selected compounds measured over the Alberta oil sands on 10 July 2008 (n=17). Samples 4–6 were collected downwind of the Syncrude Mildred Lake facility and showed the strongest enhancements for most compounds. An exception is the biogenic tracer isoprene, which was most enhanced in sample 14. CycHex=cyclohexane. Alt.=aircraft altitude (m). Maximum mixing ratios are shown in bold for each compound.

No.	Time	Lat.	Long.	Alt.	Hexane	Heptane	CycHex	Toluene	*o*-Xylene	NO_y	SO_2	C_2Cl_4	Ethane	Ethene	α-Pinene	Isoprene
1	11.05	56.887	248.822	854	16	7	10	16	0	517	190	3.39	844	54	72	457
2	11.06	56.956	248.773	838	15	5	11	13	0	889	264	2.98	833	42	79	391
3	11.07	57.027	248.714	832	17	6	12	20	4	1461	6082	3.71	884	54	130	378
4	11.08	57.079	248.608	761	141	268	47	135	94	**10 554**	**38 730**	**5.93**	**1492**	**270**	**217**	507
5	11.09	57.118	248.487	747	**294**	**596**	**133**	**401**	**127**	7343	30 976	3.77	1066	214	138	427
6	11.10	57.148	248.356	721	90	236	70	164	18	2795	1766	3.17	1106	89	31	399
7	11.11	57.123	248.236	774	13	5	12	8	0	699	299	3.22	827	95	43	344
8	11.13	56.979	248.162	794	11	4	10	9	0	259	208	2.81	794	30	17	344
9	11.15	56.905	248.174	815	6	3	6	8	0	219	190	2.74	754	23	39	363
10	11.17	56.845	248.257	846	7	5	6	8	0	231	140	2.82	809	28	15	466
11	11.20	56.785	248.348	842	10	5	8	8	0	236	119	2.79	881	42	63	768
12	11.22	56.725	248.444	843	6	3	6	6	0	211	130	2.76	797	27	42	466
13	11.24	56.665	248.532	802	10	0	5	8	0	240	130	2.71	850	31	46	677
14	11.26	56.607	248.620	787	16	7	9	9	0	296	154	2.77	902	38	55	**780**
15	11.29	56.574	248.741	785	41	14	19	12	0	645	157	2.90	940	47	48	455
16	11.32	56.564	248.876	804	37	13	16	12	0	579	174	2.79	944	50	68	496
17	11.34	56.601	248.989	817	17	7	10	8	0	373	135	2.82	874	37	28	243

Table 3. Correlation matrix for selected VOC species measured over oil sands mining operations in Alberta on 10 July 2008 (n=17). Correlations ≥0.7 are highlighted in bold. With the exception of $CHCl_3$ and C_2Cl_4, all the halocarbons showed $0.00 \leq r^2 \leq 0.43$ with the selected species and are not included.

	SO_2	NO	Ethene	Propane	*n*-Butane	Heptane	Toluene	MeCyHex
SO_2	**1.00**	**0.97**	**0.92**	**0.76**	**0.79**	0.66	0.57	0.43
NO	**0.97**	**1.00**	**0.95**	**0.82**	**0.77**	0.68	0.57	0.46
NO_2	**0.96**	**1.00**	**0.95**	**0.83**	**0.77**	0.67	0.57	0.43
NO_y	**0.96**	**1.00**	**0.96**	**0.83**	**0.77**	0.67	0.57	0.46
O_3	0.39	0.44	0.51	0.68	0.54	0.38	0.35	0.32
CO_2	0.64	**0.70**	**0.74**	0.62	0.66	**0.70**	0.66	0.60
CH_4	0.24	0.37	0.39	0.57	0.39	0.48	0.46	0.53
CO	0.63	0.57	0.60	0.59	**0.90**	**0.92**	**0.93**	**0.85**
Ethane	0.69	**0.81**	**0.77**	**0.84**	0.54	0.41	0.32	0.26
Propane	**0.76**	**0.82**	**0.82**	**1.00**	**0.84**	0.69	0.61	0.55
i-Butane	**0.81**	**0.81**	**0.82**	**0.88**	**0.99**	**0.86**	**0.80**	**0.71**
n-Butane	**0.79**	**0.77**	**0.79**	**0.84**	**1.00**	**0.89**	**0.85**	**0.76**
i-Pentane	0.54	0.54	0.57	**0.72**	**0.92**	**0.85**	**0.85**	**0.82**
n-Pentane	0.55	0.55	0.57	**0.70**	**0.93**	**0.88**	**0.88**	**0.85**
n-Hexane	**0.70**	0.69	**0.70**	**0.73**	**0.96**	**0.98**	**0.96**	**0.89**
n-Heptane	0.66	0.68	0.67	0.69	**0.89**	**1.00**	**0.99**	**0.94**
n-Octane	0.57	0.61	0.61	0.65	**0.83**	**0.99**	**0.99**	**0.97**
n-Nonane	**0.72**	**0.74**	**0.72**	**0.72**	**0.89**	**0.99**	**0.96**	**0.90**
2+3-MePentane	0.65	0.66	0.68	**0.77**	**0.95**	**0.96**	**0.94**	**0.90**
2,3-DiMeButane	**0.74**	**0.78**	**0.77**	**0.84**	**0.93**	**0.90**	**0.86**	**0.80**
Ethene	**0.92**	**0.95**	**1.00**	**0.82**	**0.79**	0.67	0.58	0.46
Propene	**0.87**	**0.93**	**0.95**	**0.75**	0.61	0.48	0.38	0.28
1-Butene	0.54	**0.70**	0.67	**0.73**	0.55	0.63	0.56	0.56
i-Butene	**0.85**	**0.90**	**0.94**	**0.71**	0.62	0.52	0.43	0.32
c-2-Butene	**0.91**	**0.93**	**0.87**	0.67	0.58	0.43	0.33	0.22
t-2-Butene	0.69	**0.83**	**0.78**	**0.79**	0.65	**0.71**	0.63	0.60
1,3-Butadiene	0.58	0.64	0.57	0.40	0.21	0.10	0.05	0.01
Isoprene	0.00	0.00	0.00	0.01	0.00	0.01	0.01	0.01

Table 3. Continued.

	SO_2	NO	Ethene	Propane	*n*-Butane	Heptane	Toluene	MeCyHex
Ethyne	**0.90**	**0.92**	**0.96**	**0.83**	**0.79**	0.63	0.54	0.43
Cyclopentane	0.61	0.62	0.61	**0.73**	**0.93**	**0.94**	**0.93**	**0.90**
MeCyclopentane	0.57	0.58	0.60	0.67	**0.89**	**0.98**	**0.99**	**0.97**
Cyclohexane	0.51	0.53	0.55	0.63	**0.83**	**0.97**	**0.98**	**0.99**
MeCyclohexane	0.43	0.46	0.46	0.55	**0.76**	**0.94**	**0.98**	**1.00**
Benzene	0.60	0.64	0.64	**0.70**	**0.86**	**0.97**	**0.97**	**0.95**
Toluene	0.57	0.57	0.58	0.61	**0.85**	**0.99**	**1.00**	**0.98**
Ethylbenzene	**0.71**	0.66	0.66	0.61	**0.91**	**0.95**	**0.93**	**0.84**
m+*p*-Xylene	**0.82**	**0.79**	**0.79**	**0.71**	**0.94**	**0.95**	**0.91**	**0.80**
o-Xylene	**0.91**	**0.88**	**0.86**	**0.75**	**0.93**	**0.89**	**0.82**	**0.70**
n-Propylbenzene	**0.92**	**0.92**	**0.89**	**0.79**	**0.91**	**0.88**	**0.81**	0.69
m-Ethyltoluene	**0.97**	**0.96**	**0.95**	**0.79**	**0.86**	**0.78**	0.69	0.56
o-Ethyltoluene	**0.98**	**0.95**	**0.91**	**0.73**	**0.82**	**0.70**	0.60	0.46
p-Ethyltoluene	**0.90**	**0.90**	**0.88**	**0.79**	**0.92**	**0.90**	**0.83**	**0.72**
1,2,3-TMB	**0.99**	**0.99**	**0.94**	**0.79**	**0.76**	0.65	0.55	0.43
1,2,4-TMB	**0.99**	**0.98**	**0.95**	**0.79**	**0.82**	**0.73**	0.63	0.50
1,3,5-TMB	**0.98**	**0.96**	**0.92**	**0.73**	**0.74**	0.61	0.50	0.37
α-Pinene	**0.76**	**0.71**	0.69	0.61	0.52	0.32	0.26	0.16
β-Pinene	0.64	0.57	0.57	0.56	0.49	0.26	0.21	0.12
Methanol	0.41	0.52	0.50	0.58	0.40	0.46	0.42	0.41
Ethanol	0.21	0.25	0.31	0.18	0.18	0.22	0.22	0.20
Acetone	0.17	0.24	0.38	0.36	0.29	0.33	0.32	0.34
MEK	**0.76**	**0.85**	**0.85**	**0.81**	0.62	0.52	0.43	0.36
MAC	0.27	0.31	0.50	0.31	0.25	0.22	0.19	0.16
MVK	0.43	0.44	0.60	0.42	0.35	0.29	0.25	0.20
$CHCl_3$	0.52	0.54	0.60	0.66	**0.80**	**0.85**	**0.86**	**0.85**
C_2Cl_4	**0.78**	**0.81**	**0.79**	0.60	0.43	0.29	0.21	0.13
OCS	0.20	0.19	0.21	0.06	0.03	0.05	0.04	0.02
DMS	0.50	0.56	0.63	0.54	0.46	0.50	0.47	0.44

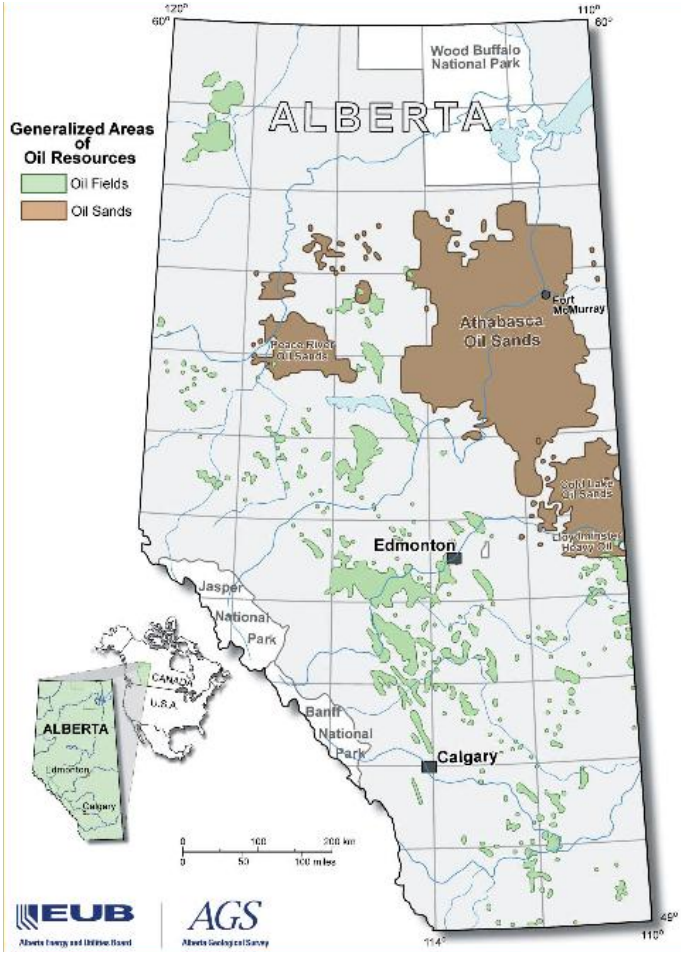

Fig. 1. Alberta's oil sands deposits in the Athabasca, Peace River, and Cold Lake regions (brown areas) (http://www.energy.alberta.ca/Oil/pdfs/oil_resources_Map.pdf).

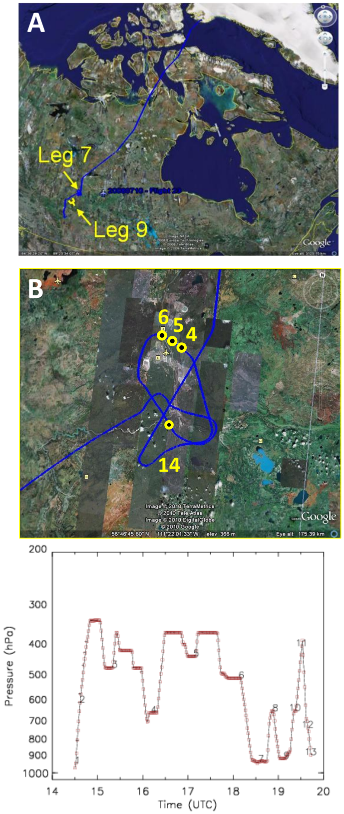

Fig. 2. (A) Flight track of the NASA DC-8 aircraft during Flight 23, a transit flight from Thule, Greenland to Cold Lake, Alberta on 10 July 2008. The DC-8 circled within the boundary layer over the oil sands for 17 min (Leg 7) then descended back into background boundary layer air 16 min later (Leg 9). **(B)** Detail of the flight path during Leg 7. The locations of selected samples shown in Table 2 are highlighted in yellow. **(C)** Vertical flight track of the aircraft during Flight 23, including Legs 7 and 9 (http://fuelberg.met.fsu.edu/research/arctas/traj/traj.html).

Title Page
Abstract | Introduction
Conclusions | References
Tables | Figures
◀| |▶
◀ ▶
Back | Close
Full Screen / Esc
Printer-friendly Version
Interactive Discussion

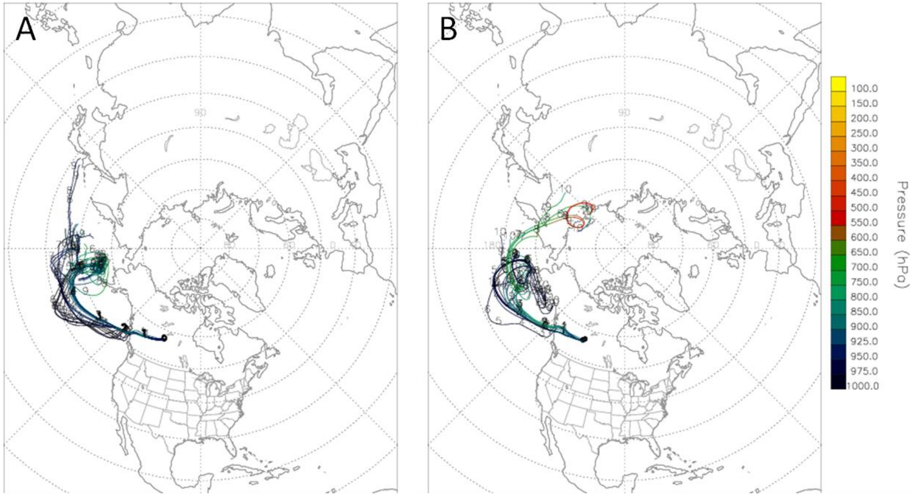

Fig. 3. Ten-day backward kinematic trajectory plots starting at flight level pressure for the two boundary layer excursions flown on 10 July 2008 **(A)** over the Alberta oil sands from 11:27–11:44 a.m. LT, i.e., Leg 7, and **(B)** in background boundary layer air from 12:00–12:14 LT, i.e., Leg 9. Computational details are given in Fuelberg et al. (2010).

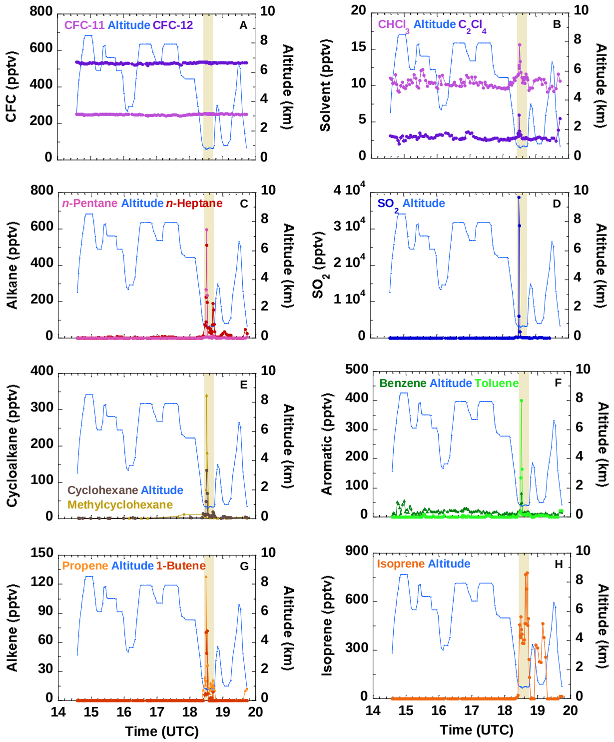

Fig. 4. Time series of selected trace gases measured during ARCTAS Flight 23 on 10 July 2008. The boundary layer run over oil sands mining operations (shaded) is followed by a second boundary run in cleaner air 1° further south (see text).

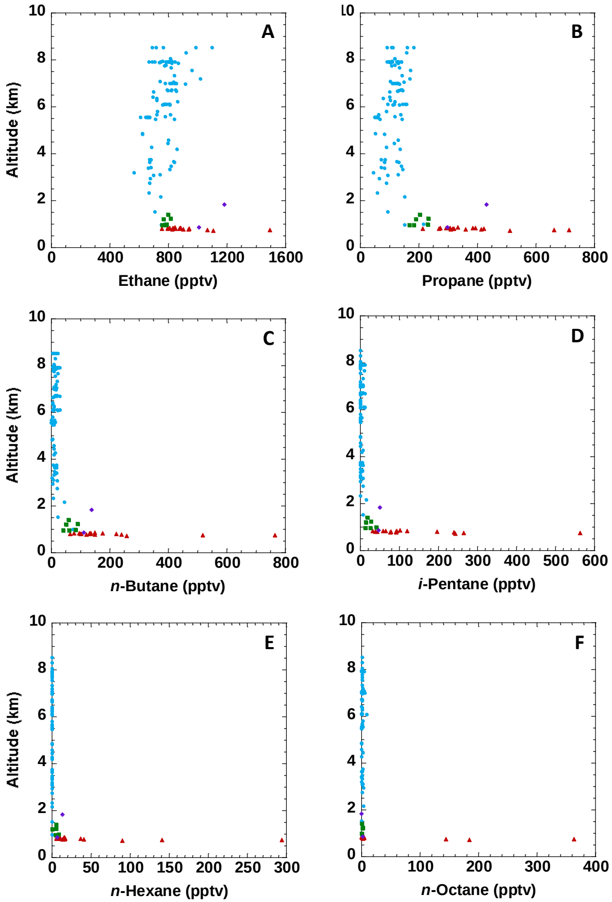

Fig. 5. Vertical profiles of selected alkanes measured during Flight 23 on 10 July 2008. Red triangles: oil sands boundary layer run (Leg 7); green squares: background boundary layer run (Leg 9); purple diamonds: Cold Lake landing; blue circles: remainder of Flight 23.

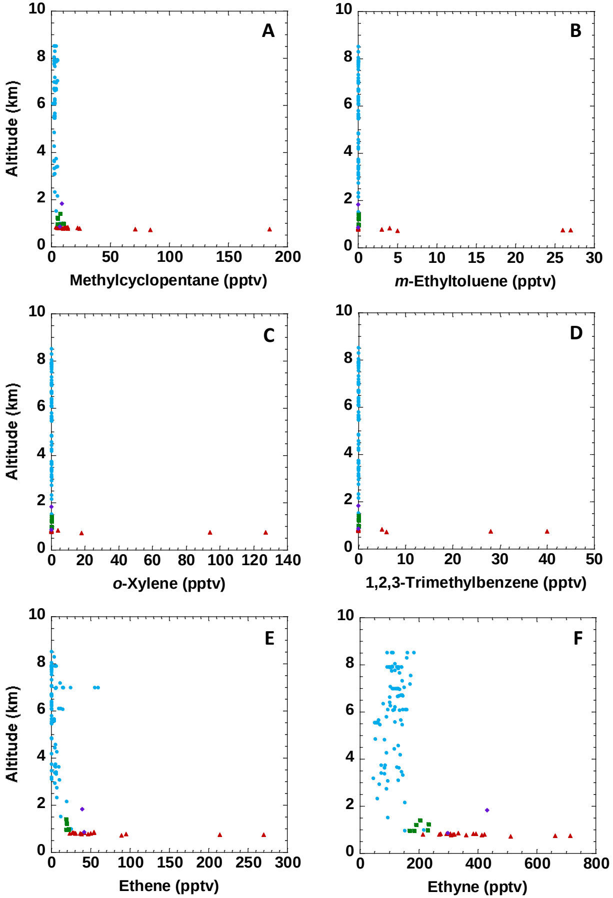

Fig. 6. As in Fig. 5 but for methylcyclopentane, selected aromatics, ethene and ethyne.

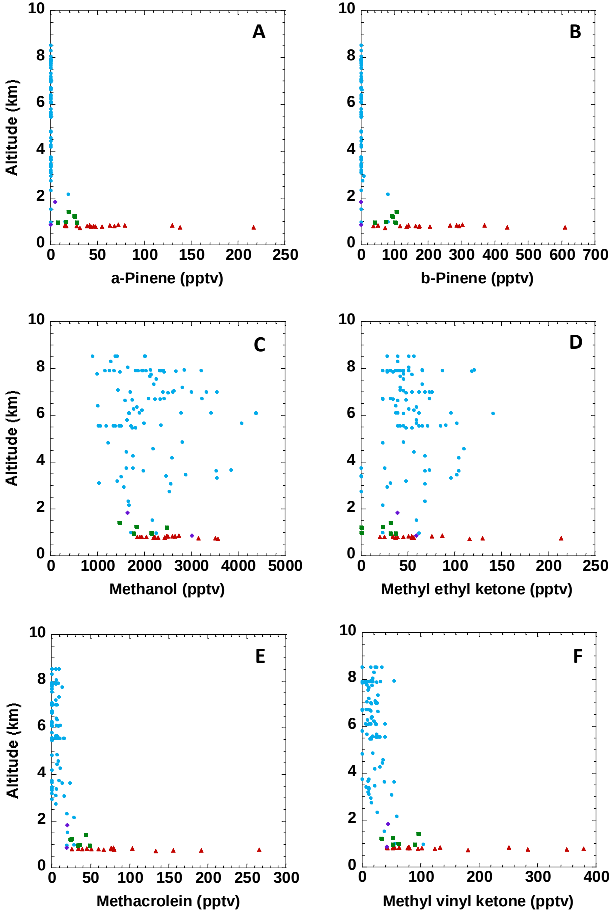

Fig. 7. As in Fig. 5 but for the pinenes and selected oxygenates.

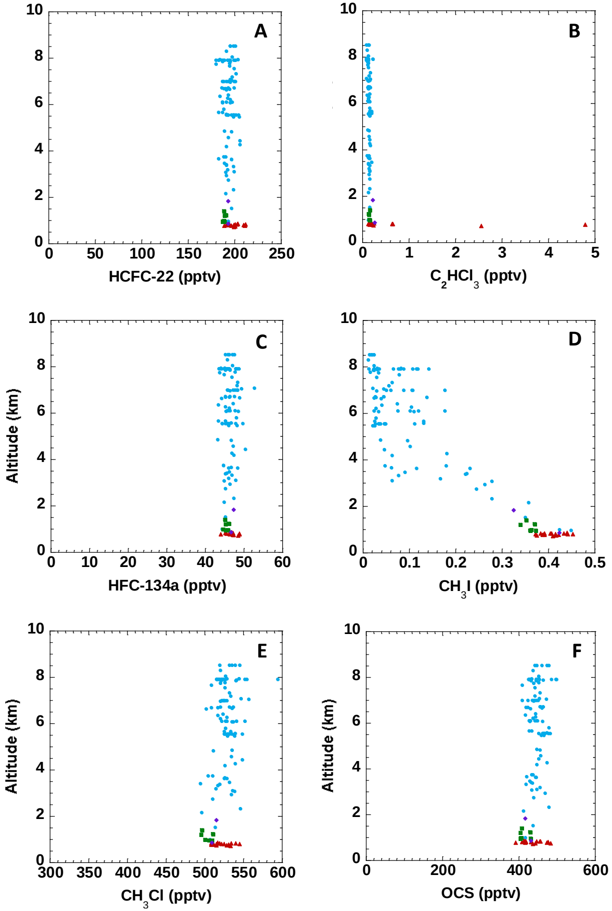

Fig. 8. As in Fig. 5 but for selected halocarbons and OCS.

Title Page
Abstract
Introduction
Conclusions
References
Tables
Figures
◀▌
▶▌
◀
▶
Back
Close
Full Screen / Esc
Printer-friendly Version
Interactive Discussion

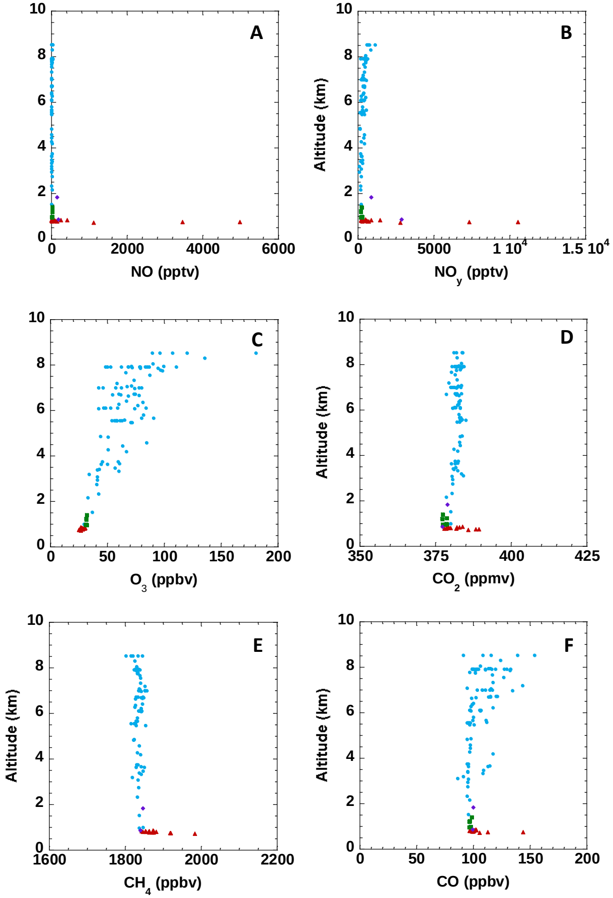

Fig. 9. As in Fig. 5 but for **(A)** NO, **(B)** NO$_y$, **(C)** O$_3$, **(D)** CO$_2$, **(E)** CH$_4$, and **(F)** CO.

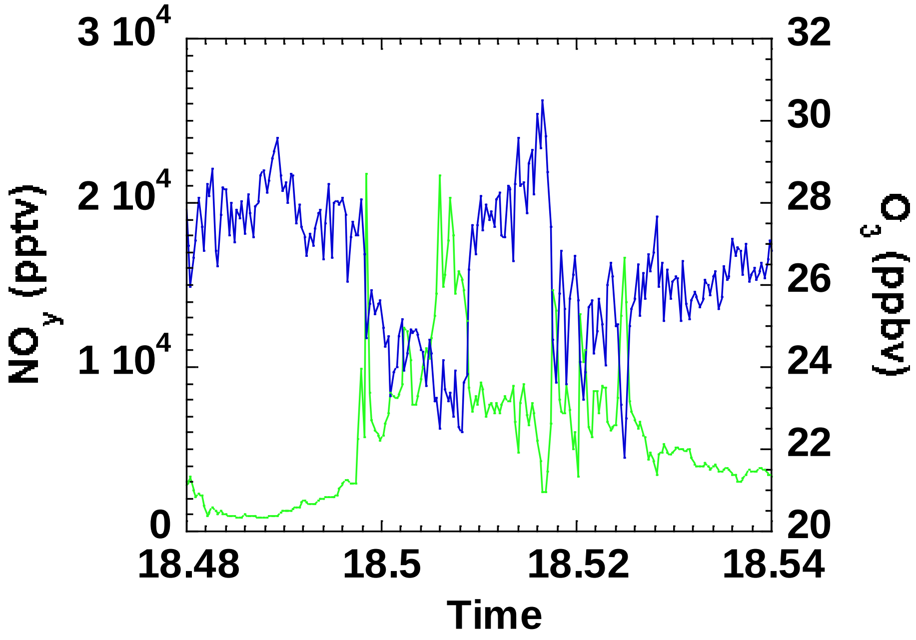

Fig. 10. Time series of NO_y (green) and O_3 (blue) over the oil sands, showing an anti-correlation between O_3 and NO_y.